*Human Molecular Genetics, 2004, Vol. 13, No. 13* **1389–1405**
*DOI: 10.1093/hmg/ddh144*
*Advance Access published on April 28, 2004*

# Progressive decrease in chaperone protein levels in a mouse model of Huntington's disease and induction of stress proteins as a therapeutic approach

**David G. Hay[1,†], Kirupa Sathasivam[1], Sönke Tobaben[2], Bernd Stahl[3], Michael Marber[4], Ruben Mestril[5], Amarbirpal Mahal[1,‡], Donna L. Smith[1,#], Ben Woodman[1] and Gillian P. Bates[1,*]**

[1]Medical and Molecular Genetics, GKT School of Medicine, King's College, London SE1 9RT, UK, [2]Molecular Design Limited, 60486 Frankfurt, Germany, [3]Institute for Molecular Biology and Cancer Research, University of Marburg, 35033 Marburg, Germany, [4]Department of Cardiology, GKT School of Medicine, King's College, London SE1 7EH, UK and [5]Department of Physiology, Loyola University, Maywood, IL 60153, USA

Received March 24, 2004; Revised and Accepted April 21, 2004

**The manipulation of chaperone levels has been shown to inhibit aggregation and/or rescue cell death in *Saccharomyces cerevisiae, Caenorhabditis elegans*, *Drosophila melanogaster* and cell culture models of Huntington's disease (HD) and other polyglutamine (polyQ) disorders. We show here that a progressive decrease in Hdj1, Hdj2, Hsp70, αSGT and βSGT brain levels likely contributes to disease pathogenesis in the R6/2 mouse model of HD. Despite a predominantly extranuclear location, Hdj1, Hdj2, Hsc70, αSGT and βSGT were found to co-localize with nuclear but not with extranuclear aggregates. Quantification of Hdj1 and αSGT mRNA levels showed that these do not change and therefore the decrease in protein levels may be a consequence of their sequestration to aggregates, or an increase in protein turnover, possibly as a consequence of their relocation to the nucleus. We have used genetic and pharmacological approaches to assess the therapeutic potential of chaperone manipulation. Ubiquitous overexpression of Hsp70 in the R6/2 mouse (as a result of crossing to Hsp70 transgenics) delays aggregate formation by 1 week, has no effect on the detergent solubility of aggregates and does not alter the course of the neurological phenotype. We used an organotypic slice culture assay to show that pharmacological induction of the heat shock response might be a more useful approach. Radicicol and geldanamycin could both maintain chaperone induction for at least 3 weeks and alter the detergent soluble properties of polyQ aggregates over this time course.**

## INTRODUCTION

Nine inherited late-onset neurodegenerative disorders, including Huntington's disease (HD), dentatorubral pallidoluysian atrophy (DRPLA), the spinocerebellar ataxias (SCA) 1, 2, 3, 6, 7 and 17, and spinal and bulbar muscular atrophy (SBMA) are caused by a CAG/polyglutamine (polyQ) repeat expansion (1). In all cases the neuropathology of these diseases is characterized by the presence of nuclear, and in some cases extranuclear, aggregates that are immunoreactive for the mutant protein and for ubiquitin. Although it is likely that the misfolding and accumulation of mutant polyQ is central to the pathogenesis of these diseases, the structures of the intermediates involved in aggregate formation, the stage at which

*To whom correspondence should be addressed at: Medical and Molecular Genetics, GKT School of Medicine, King's College London, 8th Floor Guy's Tower, Guy's Hospital, London SE1 9RT, UK. Tel: +44 2071883722; Fax: +44 2071883727; Email: gillian.bates@genetics.kcl.ac.uk
[†]Present address: CRUK Tumour Cytokine Biology Group, Wolfson Digestive Disease Centre, University Hospital, Nottingham NG7 2UH, UK.
[‡]Present address: MRC Clinical Sciences Centre, Faculty of Medicine, Imperial College, London W12 0NN, UK.
[#]Present address: Department of Pathology, College of Physicians and Surgeons, Columbia University, New York, NY 10032, USA.

 

this process is first detrimental to cells and the relationship of the aggregation process to neuronal dysfunction and neuronal cell death is not understood (2–4).

Chaperones assist proteins in folding into their native conformation, refold abnormally folded proteins and rescue previously aggregated proteins (5,6). For example, the Hsp70 chaperones promote protein folding by an ATP-dependent process and work in concert with their Hsp40 co-chaperones, which recognize non-native polypeptide segments, target them to Hsp70 and at the same time activate the Hsp70 ATPase. Proteins that cannot be refolded are marked for degradation by the covalent attachment of a polyubiquitin chain (7), enabling the protein to be recognized and hydrolysed by the 26S proteasome (8). Members of the Hsp40 (Hdj1 and Hdj2) and Hsp70 (Hsc70 and Hsp70) chaperone families have been found to co-localize with nuclear aggregates in SCA 1 (9) and SCA3 (10,11) autopsy patient brains and SCA1 (9), SCA7 (12) and HD (13) transgenic mouse brains. In addition, Hsp84 co-localizes with nuclear aggregates in HD transgenic mouse brains (14) and Hsp105α in SBMA autopsy brains and transgenic mouse brains (15). The recruitment of chaperones to polyQ aggregates, along with components of the 20S, 19S and 11S proteasome complexes (9–12) indicates that the polyQ tracts have been recognized as misfolded conformers and that the cell has been unsuccessful in attempts to prevent their accumulation (16,17).

Modulation of molecular chaperone levels can promote the refolding of polyQ aggregates or their ubiquitin-dependent degradation and this has been extensively explored using mammalian cell models of polyQ disease. Members of the Hsp40 and Hsp70 chaperone families have been shown to inhibit aggregate formation (9,10,13,18–22) and prevent cell toxicity (13,19,20), an effect that is enhanced when Hsp40 and Hsp70 chaperones are overexpressed in combination and can work synergistically (13,19,20,22). As a step toward exploiting this therapeutically, Sittler *et al.* (20) have successfully demonstrated that geldanamycin (GA), a benzoquinone ansamycin that binds to Hsp90 and activates the stress response, can be used to induce expression of Hsp40 and Hsp70 and inhibit polyQ aggregation in a dose-dependent manner (20). However, the relative effects of the Hsp40 and Hsp70 chaperones do differ from one polyQ disease model to another; in one report overexpression of Hdj2 was found to increase aggregation (23), and in another, the suppression of toxicity was linked to the ability of the chaperones to inhibit caspase activation rather than aggregation (21). Inhibition of polyQ aggregation and toxicity in mammalian cell models has also been achieved through the overexpression of Hsp84 (14), Hsp105a (15) and the DnaJ-like protein, MRJ (24) and even by the use of fragments of the bacterial chaperone GroEL and the full-length yeast Hsp104 (25). Hsp27 also suppresses toxicity although this was shown to act by reducing reactive oxygen species and protecting against oxidative stress, rather than by inhibiting aggregate formation (26).

The modulation of chaperone levels has also been used to delay the onset and progression of polyQ-induced phenotypes and neurodegeneration in *Caenorhabditis elegans* (27) and *Drosophila* (28–31) models of polyQ disease, but has had mixed success in modulating phenotype progression in mouse models (32–34). As in cell culture systems, Hsp40 and Hsp70 acted synergistically in their suppression of neurotoxicity in a *Drosophila* model of SCA3 (29). In this case, suppression of neurodegeneration was shown to correlate with an increase in the solubility of the polyQ aggregates (28,29), which was consistent with experiments in yeast in which co-expression of Hsp40 and Hsp70 or of Hsp104 promoted the accumulation of detergent soluble aggregates instead of detergent insoluble polyQ inclusions (35,36). *In vitro*, Hsp70 and Hsp40 could be shown to suppress the assembly of expanded polyQ into detergent-insoluble amyloid-like fibrils in an ATP-dependent manner and caused the formation of amorphous, detergent-soluble aggregates thereby altering their biochemical properties (35).

We have used the R6/2 mouse model of HD to investigate the extent to which a reduction in chaperone levels might contribute to or accelerate the pathogenesis of this disease. We have found that brain levels of Hdj1, Hsp70, αSGT and βSGT (small glutamine-rich tetratricopeptide repeat containing proteins) progressively decrease to $<40\%$ of the endogenous levels by 14 weeks. This decrease in soluble protein levels is not caused by a decrease in the transcription of these genes but correlates with the recruitment of the chaperone protein into nuclear aggregates. We have used an organotypic slice culture assay to show that the overexpression of Hsp70 in the R6/2 mouse (by crossing to mice transgenic for Hsp70) leads to an early but only transient decrease in aggregate formation. To assess the therapeutic potential of chemical compounds that result in a stress protein induction, we have used radicicol (RA) and GA in the organotypic slice culture assay. It was possible to maintain chaperone induction over a period of 3 weeks and although aggregate formation was only delayed transiently, the levels of the soluble huntingtin transgene protein remained significantly increased, suggesting that the preclinical testing of a compound that induces the heat shock response and crosses the blood–brain barrier is warranted.

## RESULTS

### Progressive decrease of specific chaperone levels in the R6/2 mouse brain

The R6/2 mouse model of HD expresses exon 1 of the human HD gene (37,38) with approximately 200 CAG repeats (39). PolyQ aggregates can be detected in the brain prior to 4 weeks of age (40,41), a behavioural phenotype is apparent by 6 weeks (42,43) and the disease progresses rapidly such that mice are rarely kept beyond 14 weeks. In order to investigate whether a decrease in chaperone levels might contribute to pathogenesis in the R6/2 mouse model, we compared the protein levels and subcellular localization of a wide range of chaperones in R6/2 and wild-type mice. Western blots of whole brain lysates from R6/2 mice aged 14 weeks were immunoprobed with antibodies to the small heat shock proteins: αB-crystallin and Hsp25; members of the Hsp40 family: Hdj1 and Hdj2; the Hsp70 family: Hsc70, Hsp70 and Grp78; the Hsp90 family: Hsp90 and Hsp84; as well as cysteine string protein (CSP); the small glutamine-rich tetratricopeptide repeat containing proteins: αSGT and βSGT; and p60 (HOP: Hsp organizing protein). At 14 weeks, levels

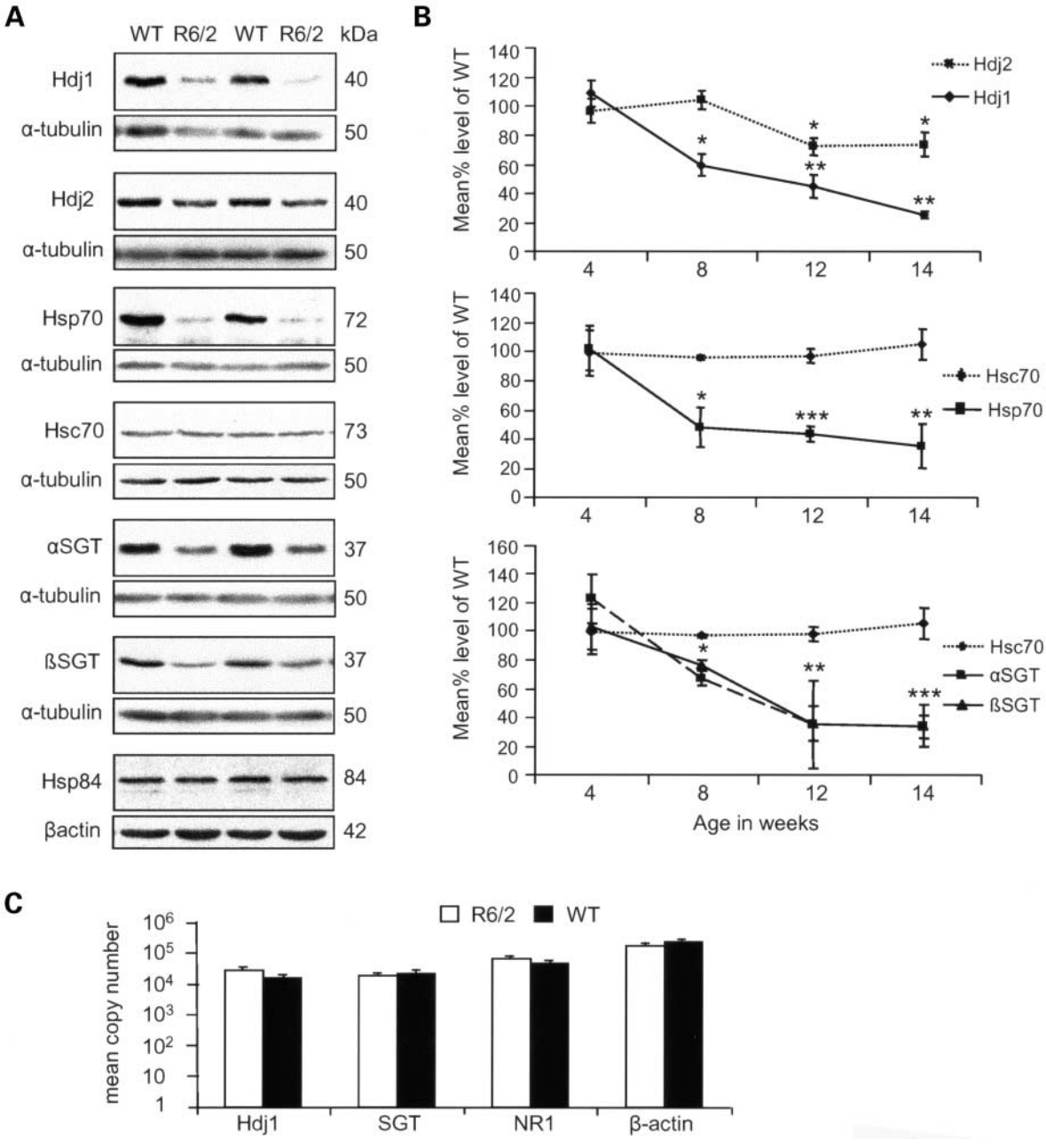


**Figure 1.** Progressive decrease in chaperone levels may contribute to R6/2 pathogenesis. (**A**) Western blots of whole brain lysates from wild-type (WT) and R6/2 mice at 14 weeks of age. Hdj1, Hdj2, Hsp70, αSGT and βSGT levels are decreased in R6/2 brains whereas Hsc70 and Hsp84 levels remain unchanged. Blots were reprobed with antibodies to α-tubulin or β-actin to show relative loading levels. (**B**) Quantification of the progressive decrease in chaperone levels in R6/2 brains when compared with wild-type over the course of the R6/2 lifespan. Each data point arises from a comparison of five R6/2 and five wild-type mice. (**C**) Real-time PCR quantification shows no difference in the mRNA levels of Hdj1 and SGT between R6/2 and wild-type mice. NR1 [glutamate (NMDA) receptor subunit zeta 1 precursor] and β-actin mRNAs were quantified as controls. Error bars represent standard errors of the mean; $^{*}P \leq 0.05$, $^{**}P \leq 0.01$, $^{***}P \leq 0.001$.

of Hdj1, Hdj2, Hsp70, αSGT and βSGT were decreased (Fig. 1A), whereas αB-crystallin, Hsp25, Hsc70, Grp78, Hsp90, Hsp84, CSP, and p60 remained unchanged (Fig. 1A and data not shown). Therefore, we did not confirm the decrease in αB-crystallin levels previously detected by 2D gel electrophoresis (44). To determine the time course over which the chaperone levels decreased, western blotting was repeated with whole brain lysates from wild-type and R6/2 mice ($n = 5$) aged 4, 8 and 12 weeks and immunoprobed with antibodies to Hdj1, Hdj2, Hsp70, αSGT and βSGT. Semi-quantitative analysis indicated that Hdj1, Hsp70, αSGT and βSGT levels were significantly decreased by 8 weeks of age and in all cases, these had decreased to $<40\%$ of wild-type levels by 12 weeks (Fig. 1B). The decrease in Hdj2 levels was less pronounced, reaching significance at 12 weeks of age and remaining $<75\%$ of wild-type levels at 14 weeks.

### Expression changes are at the level of the protein and not the RNA

Transcriptional dysregulation is a feature of the molecular pathogenesis in HD (45–47) and has been described in patient brains and in the R6/2 mice (48,49). In order to determine whether the decrease in protein levels of specific chaperones might be a consequence of a decrease in mRNA levels, real-time PCR was performed for αSGT and Hdj1. We were unable to establish a real-time PCR assay for Hsp70. cDNA was prepared from R6/2 and wild-type brains from mice at 14 weeks of age ($n = 5$). The mean copy number of transcripts was determined for αSGT and for Hdj1 and compared with that of the glutamate (NMDA) receptor subunit zeta 1 precursor (NR1) and β-actin as controls (Fig. 1C). There was no difference in the mRNA levels of αSGT and Hdj1 between wild-type and R6/2 brains at 14 weeks.

### Specific chaperones are recruited into nuclear but not into extranuclear aggregates

In order to examine whether the subcellular localization of chaperones was altered in the R6/2 mouse brain, immunohistochemistry was performed on coronal sections from 14 week R6/2 and wild-type mice with antibodies to αB-crystallin, Hsp25, Hdj1, Hdj2, Hsc70, Hsp70, Grp78, Hsp90, Hsp84, CSP, αSGT, βSGT and p60, and the pattern of staining was examined in the cerebral cortex, striatum and hippocampus. Antibodies to Hdj1, Hdj2, Hsc70, αSGT and βSGT detected a single puncta resembling a nuclear inclusion in all three brain regions from R6/2 mice but not in the wild-type controls (Fig. 2A). There was no difference in the localization of αB-crystallin, Hsp25, Grp78, Hsp90, Hsp84 and p60 between R6/2 and wild-type and staining could not be detected with antibodies to Hsp70 and CSP. Therefore, we did not replicate the previous finding that Hsp84 co-localizes with nuclear inclusions in the R6/2 brain (14). To test whether the chaperones were co-localized with polyQ aggregates, we performed double labelling and confocal microscopy. Antibodies to Hdj1, Hdj2, Hsc70, αSGT and βSGT all showed co-localization with nuclear inclusions detected by the anti-huntingtin antibodies EM48 or S830 in the hippocampus, striatum and cortex (Fig. 2B and data not shown) but did not co-localize with extranuclear aggregates (Fig. 2B). This is illustrated very clearly in the hippocampus, where the co-localization of these chaperones with polyQ aggregates is apparent in the nuclear inclusions in the dentate gyrus, but not with the dense and prominent extranuclear aggregates that are present in the hilius (Fig. 2B and data not shown).

To determine the time at which staining of inclusions could be detected with antibodies to Hdj1, Hdj2, Hsc70, αSGT and βSGT, immunohistochemistry was performed against R6/2 and wild-type brain sections from mice at 4, 8 and 12 weeks of age. Co-localization with Hdj2, Hsc70, αSGT and βSGT was first detected in the CA1 pyramidal cells of the hippocampus at 4 weeks and could be identified in both the cortex and striatum by 8 weeks (Table 1). Co-localization with Hdj1 was not apparent until 14 weeks, but this is likely to reflect the weak staining obtained with this antibody, rather than the age at which recruitment first occurs.

### Overexpression of Hsp70 does not improve the phenotype in the R6/2 mice

The overexpression of the chaperone Hsp70 has been shown to inhibit aggregation and/or rescue cell toxicity in an *in vitro* system (35) and in yeast (35,36), cell culture (13,19–22,35) and *Drosophila* models of polyQ disease (28). However, in order to assess the therapeutic potential of such a strategy, it is important that overexpression of Hsp70 is also shown to have beneficial effects in mouse models. Initial results were encouraging as crossing the B05 mouse model of SCA1 to mice transgenic for Hsp70 had mildly beneficial effects on the SCA1 neurological phenotype (32). Given that mutant ataxin 1 is overexpressed 50–100-fold in the B05 model (50), and only in Purkinje cells, we reasoned that overexpression of Hsp70 in a model in which the transgene is not overexpressed might show a more significant benefit.

Therefore, we elected to test the effects of crossing the R6/2 mouse model of HD to the same Hsp70 overexpressing mice as were used in the SCA1 cross. These mice (denoted Hsp70i) are transgenic for the rat Hsp70 gene driven by the chicken β-actin promoter and cytomegalovirus enhancer (51). R6/2 males were bred to Hsp70i hemizygous females so that the four genotypes used in the analysis: wild-type, R6/2, Hsp70i and double transgenic mice were derived from the same litters. Figure 3A shows western blots of whole brain lysates from mice of all four genotypes aged 4 weeks. The soluble huntingtin exon 1 protein is present in the R6/2 and double transgenic brains. Expression of Hsp70 can be detected clearly in Hsp70i and double transgenic mice. However, because endogenous levels of Hsp70 are comparatively low, the western blot would have had to have been overexposed in order to detect Hsp70 in the wild-type and R6/2 brains.

The breeding was set up such that sufficient female mice for the phenotype analysis were born over the course of 3 days. On weaning, the mice ($n = 15$ per genotype) were distributed between the cages such that each cage contained at least one mouse from each genotype, and the phenotype assessment commenced at 4 weeks of age and progressed until 12 weeks. Mice were weighed weekly, and as expected female R6/2 mice showed relative weight loss compared with wild-type mice from 10 weeks of age (10 weeks difference in weight = 1.6 g, $P = 0.005$) (Fig. 3B). The Hsp70i mice also showed a weight loss with respect to wild-type mice over this time period (10 weeks difference in weight = 1.2 g, $P = 0.029$). There was an additive effect between the R6/2 and Hsp70i genotypes and no interaction (12 weeks GLM ANOVA: $F_{1,56} = 0.11$, $P = 0.74$).

The Rotarod performance of R6/2 mice when compared with wild-type was severely impaired by 8 weeks (GLM ANOVA: $F_{1,55} = 37.75$, $P < 0.001$) and remained so at 12 weeks of age (GLM ANOVA: $F_{1,55} = 51.76$, $P < 0.001$) (Fig. 3C). There was no interaction between the R6/2 and Hsp70i genotypes at 8 weeks (GLM ANOVA: $F_{1,55} = 0.72$, $P = 0.399$) or 12 weeks of age (GLM ANOVA: $F_{1,55} = 1.11$, $P = 0.982$) and therefore, overexpression of Hsp70 did not modify the R6/2 Rotarod impairment.

Similarly, R6/2 mice displayed reduced grip strength compared with wild-type mice from 8 weeks of age (8 weeks GLM ANOVA: $F_{1,55} = 16.87$, $P < 0.001$; 12 weeks GLM ANOVA: $F_{1,55} = 70.89$, $P < 0.001$). The double transgenic mice also

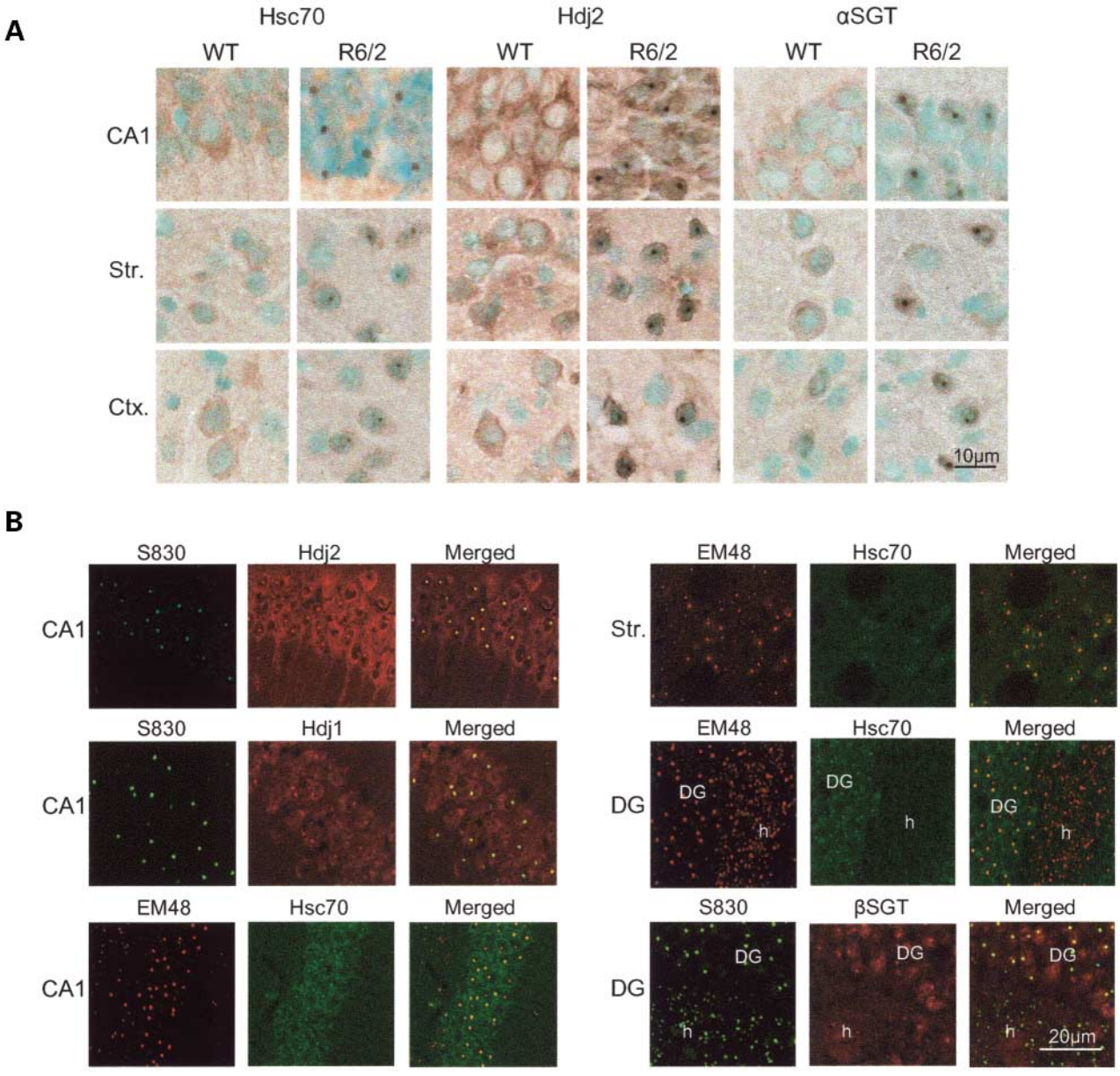


**Figure 2.** Specific chaperones are recruited to nuclear but not to extranuclear aggregates. (**A**) Localization of Hdj2, Hsc70 and αSGT in the cortex, striatum and hippocampal CA1 pyramidal neurons of wild-type (WT) and R6/2 mice. In R6/2 mice, a single puncta of staining, resembling a nuclear inclusion (NI) is also apparent in the nucleus. Methyl green was used as a nuclear counterstain. (**B**) Demonstration of co-localization of the chaperones with the NIs by confocal microscopy in R6/2 brains at 14 weeks. Co-localization of Hdj2, Hsp70, Hsc70, αSGT and βSGT with NIs was demonstrated in the hippocampus (CA1 or DG), cortex and striatum (Str.) and a selection of images are shown (left panels and top right). Extensive extranuclear aggregates are observed in the hilius (h) close to the dentate gyrus (DG) of the hippocampus in R6/2 brains. Co-localization of both Hsc70 and βSGT could be detected with NIs, but not with extranuclear aggregates (middle and bottom right panels).

developed a reduction in grip strength over this time period and there was no interaction between the R6/2 and Hsp70i genotypes (8 weeks GLM ANOVA: $F_{1,55} = 0.01$, $P = 0.941$; 12 weeks GLM ANOVA: $F_{1,55} = 0.22$, $P = 0.642$).

### Overexpression of Hsp70 has an initial inhibitory effect on polyQ aggregation

In order to quantify the effect that overexpression of Hsp70 has on the initiation of aggregate formation, we used the hippocampal slice culture assay. We have previously shown that aggregates form at the same rate and in the same sequence in hippocampal slice cultures as they do in the R6/2 mouse *in vivo* (52). Slice cultures were established from R6/2 and double transgenic mice at P7 and harvested after 2, 3 and 4 weeks in culture. All slices were immunostained in parallel with the S830 anti-huntingtin antibody and Alexa 488 conjugated secondary (Fig. 4A) and the aggregate load in each slice quantified using confocal microscopy. The number of aggregates in the slices from the double transgenic mice was

**Table 1.** Age (weeks) at which specific chaperones were first detected in the inclusions

| | Hdj1* | Hdj2 | Hsc70 | αSGT | βSGT |
|---|---|---|---|---|---|
| Striatum | 14 | 8 | 8 | 8 | 8 |
| Cortex | 14 | 8 | 4 | 8 | 8 |
| Hippocampus CA1 | 14 | 4 | 4 | 4 | 4 |

*Staining with this Hdj1 antibody is weak, and Hdj1 is most likely present in nuclear inclusions prior to 14 weeks of age.

significantly decreased after 2 weeks in culture as determined by three measurement parameters: number of aggregates ($P = 0.0001$); total fluorescence intensity ($P = 0.0002$); total aggregate area ($P = 0.0002$) (Fig. 4B). However, the effect had diminished by 3 weeks and there was no significant difference at the 3 and 4 weeks time points. Consistent with this, aggregates could be detected only rarely in CA1 neurons in hippocampal sections from double transgenic mice aged 3 weeks (equivalent to 2 weeks in slice culture), whereas they were already apparent in R6/2 sections (Fig. 4C). At 4 weeks of age (equivalent to 3 weeks in slice culture) aggregates were present in the CA1 pyramidal neurons from both genotypes. Therefore, overexpression of Hsp70 in the R6/2 mouse results in an early but transient inhibition of aggregate formation.

We failed to detect any other differences between the progression of the molecular pathology in the R6/2 and double transgenic mice. There was no apparent difference in aggregate load in brain sections at 8 weeks (Fig. 5A) and 12 weeks of age (data not shown). Owing to low levels of expression, it had not been possible to detect Hsp70 immunostaining in brain sections from wild-type and R6/2 mice but this was easily detectable in Hsp70i and double transgenic brain sections (data not shown) in which recruitment of Hsp70 to nuclear inclusions could be detected by 8 weeks of age (Fig. 5B). Overexpression of Hsp70 did not increase levels of soluble huntingtin exon 1 in the double transgenic mice from 4 weeks of age onwards (Fig. 5C and data not shown) and had no effect on the progressive decrease of Hdj1, Hdj2, Hsc70, αSGT and βSGT (Fig. 5C and data not shown). In fact, the level of Hsp70 expressed from the transgene also decreased progressively in the double transgenic mice when compared with the Hsp70i mice (12 weeks, $n = 3$, $P = 0.0018$) (Fig. 5D). As it has been shown previously that Hdj1 and Hsp70 act synergistically to prevent polyQ fibril formation and/or cell toxicity (19,20,22,29), a reduction in the levels of Hdj1, Hdj2 and other chaperones might compromise the beneficial effects of Hsp70 overexpression.

### GA and RA induce the heat shock response in an organotypic slice culture

The administration of compounds such as GA can be used to induce a heat shock response and thereby increase expression of both Hdj1 and Hsp70 in parallel. GA is a benzoquinone ansamycin that binds specifically to the ATP/ADP binding site of Hsp90, disrupting the complex that represses heat shock factor 1 (HSF1) and thereby releasing HSF1 and inducing expression of Hdj1 and Hsp70. GA has been shown to inhibit aggregation of huntingtin exon 1 protein in a cell culture model (20) and more recently was shown to rescue degeneration of dopaminergic neurons in a *Drosophila* model of Parkinson's disease (53). Therefore, we used the hippocampal slice culture system to assess how successful such compounds might be as therapeutics in a mouse model of HD, and whether the co-induction of Hdj1 and Hsp70 might be more successful at attenuating aggregation and increasing soluble levels of huntingtin exon 1 protein than the overexpression of Hsp70 alone. We chose three compounds for analysis: GA, RA and pyrollidine dithiocarbamate (PDTC). RA is a fungal macrocyclic antibiotic that induces the heat shock by the same mechanism as GA, with which it shares the same Hsp90 binding site (54). PDTC is a low molecular weight thiol compound with anti-oxidant activities, which has been shown to induce HSF1 activation and heat shock protein expression in rat fibroblast cells by an unknown mechanism (55).

First we set out to ensure that the organotypic slice culture procedure did not itself induce a stress response. Hippocampal slices were cultured from P7 neonates and lysates prepared for western blotting after 0, 2, 4 and 7 days in culture. Hsp70 levels were barely detectable indicating that a heat shock response had not been induced (data not shown), a result that was subsequently reproduced in an extensive number of control slice cultures. Next, we exposed slices to GA, RA and PDTC and asked what concentrations, if any, induced a heat shock response in the slice cultures. Slices were cultured for 7 days and then either remained untreated or were exposed to vehicle or varying concentrations of a given drug for 48 h before processing for western blotting. GA was added to the cultures at 1 nM, 10 nM, 100 nM, 1 μM and 10 μM, and concentrations above 100 nM proved to be toxic. RA was tested over the 4-log concentration range: 100 nM to 100 μM, and 100 μM was found to be toxic, and PDTC was tested from 10 μM to 10 mM, with 10 mM proving to be toxic. PDTC failed to induce expression of Hdj1 or Hsp70 at any of the concentrations tested. In contrast, 100 nM GA and 10 μM RA both induced expression of Hdj1 and Hsp70, but not of the four other chaperones that were tested: Hsp25, Hsc70, Hsp90 and αSGT (Fig. 6A and data not shown). A semi-quantitative analysis of western blots of treated and untreated samples ($n = 4$) indicated that Hdj1 levels were increased ~4- and 5-fold by treatment with 100 nM GA and 10 μM RA, respectively (Fig. 6B). The extent of Hsp70 induction could not easily be quantified as endogenous levels were so low, but a marked induction was apparent both by western blot analysis (Fig. 6A) and by immunohistochemistry of treated and untreated slices (Fig. 6C).

Prior to assessing the effects of treating the slice cultures with 100 nM GA and 10 μM RA, we monitored the extent of heat shock induction over a period of 3 weeks in response to 'constant' and 'pulsed' dosing regimes. First we established that exposure of the slices to 10 μM RA for 8 h induced an equivalent heat shock to that in slices that had been exposed to 10 μM RA for 48 h (data not shown). Slices were established from R6/2 neonates at P7 and cultured for 1 week after which either: (1) 10 μM RA was added to the medium and then replenished when the medium was changed twice

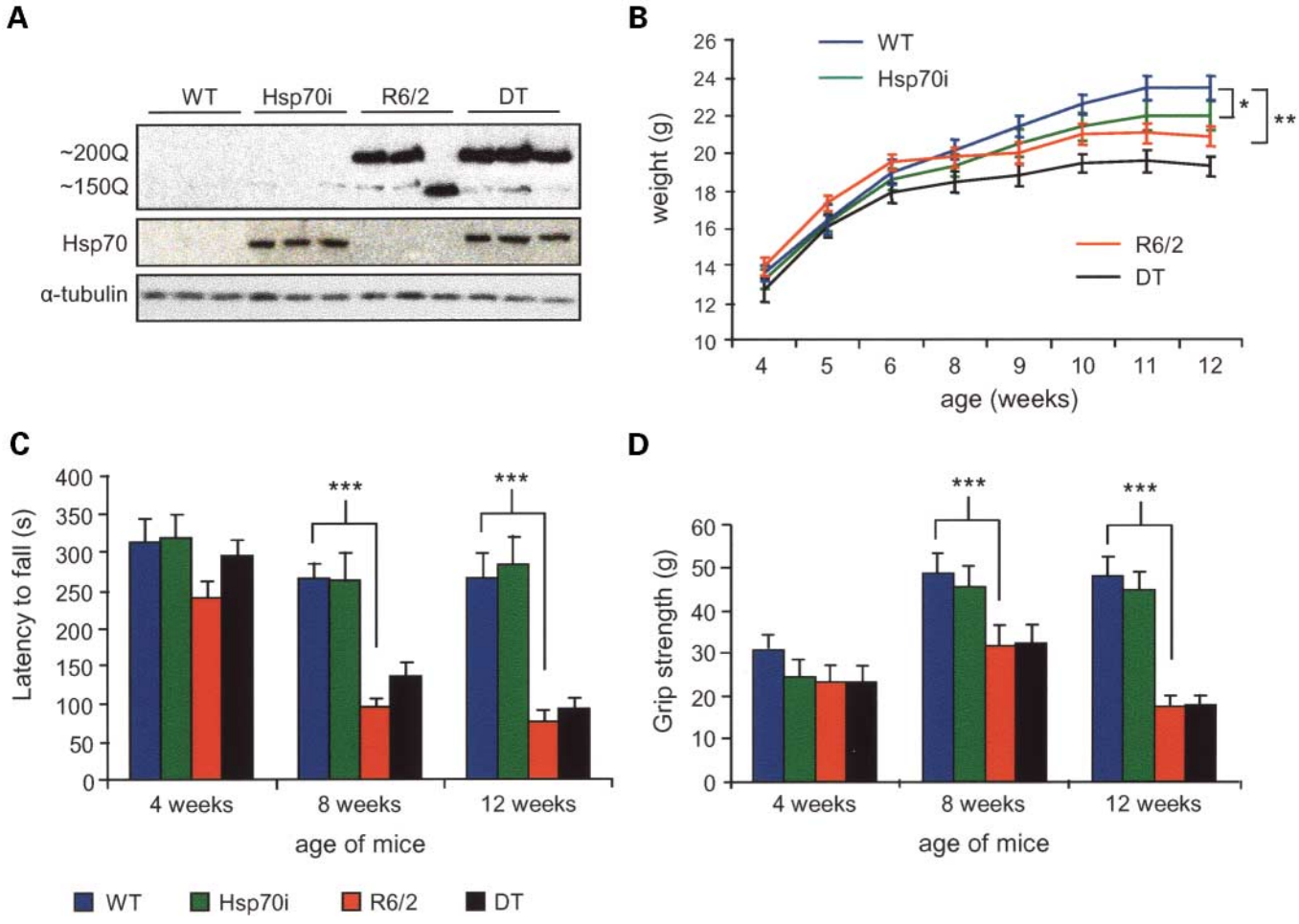


**Figure 3.** Phenotype analysis of mice that are double transgenic for the R6/2 and Hsp70 transgenes. (**A**) Western blot of whole brain lysates from wild-type (WT), Hsp70i, R6/2 and double transgenic (DT) mice at 4 weeks of age. The top panel shows the HD exon 1 transgene protein as detected with the S830 antibody. A contraction has occurred in the CAG repeat carried by one of the R6/2 mice such that the polyQ tract has decreased to approximately 150Q from approximately 200Q. Repeat contractions such as this are very rare and have been identified in <0.05% of the R6/2 mice that we have repeat sized (unpublished data). The expression of Hsp70 from the Hsp70 transgene (Hsp70i) can be seen in the middle panel. Because of the low expression of endogenous Hsp70, it was not possible to quantify the degree to which Hsp70 is overexpressed in these mice. The blot was reprobed with α-tubulin (bottom panel) to show relative loading levels. (**B**) There is a significant decrease in weight gain in the Hsp70i mice when compared with wild-type. Both the R6/2 and double transgenic mice show an impaired weight gain compared with wild-type. There is no interaction between weight gain and the R6/2 and Hsp70 transgenes. (**C**) RotaRod performance in the double transgenic mice is not significantly improved when compared with R6/2. (**D**) Grip strength in the double transgenic mice is not significantly improved when compared with R6/2. Error bars represent standard errors of the mean; $^{*}P \leq 0.05$, $^{**}P \leq 0.01$, $^{***}P \leq 0.001$.

weekly; or (2) 10 μM RA was added to the medium for 8 h, removed and replaced with fresh medium, and this pulsed dosing was repeated every 4 days. Slices were harvested after 2, 3 and 4 weeks in culture (i.e after 1, 2 and 3 weeks exposure to either of the dosing regimes). Slices that had been exposed to 10 μM RA for 48 h, a treatment known to induce heat shock, were used as a positive control. Both of the dosing regimes were successful in maintaining a heat shock response over the course of the experiment (Fig. 6D). Quantification of Hdj1 induction when compared with the vehicle control indicated that constant exposure to 10 μM RA induced and maintained higher levels of Hdj1 when compared with the pulsed regime (Student's *t*-test, $n = 3$, 2 weeks: constant $P = 0.004$, pulsed $P = 0.49$; 3 weeks: constant $P < 0.001$, pulsed $P = 0.02$; 4 weeks: constant $P = 0.04$, pulsed $P = 0.01$).

### Pharmacological induction of the heat shock response does not maintain inhibition of aggregation but does render aggregates more detergent soluble

In order to assess the therapeutic potential of RA, slice cultures were exposed to vehicle or to 100 nM, 1 μM or 10 μM RA after 7 days in culture and harvested after they had been cultured for a=total of 2, 3 and 4 weeks. All slices were sectioned and immunostained in parallel with the S830 anti-huntingtin antibody and Alexa 488 conjugated secondary and the aggregate load in each slice quantified using confocal microscopy as before. Exposure to 100 nM and 1 μM RA had no effect on the formation of aggregates in the slices over the course of the experiment (data not shown). In contrast, treatment with 10 μM RA caused a statistically significant decrease in the aggregate load after 2 weeks in culture (1 week of treatment) by each

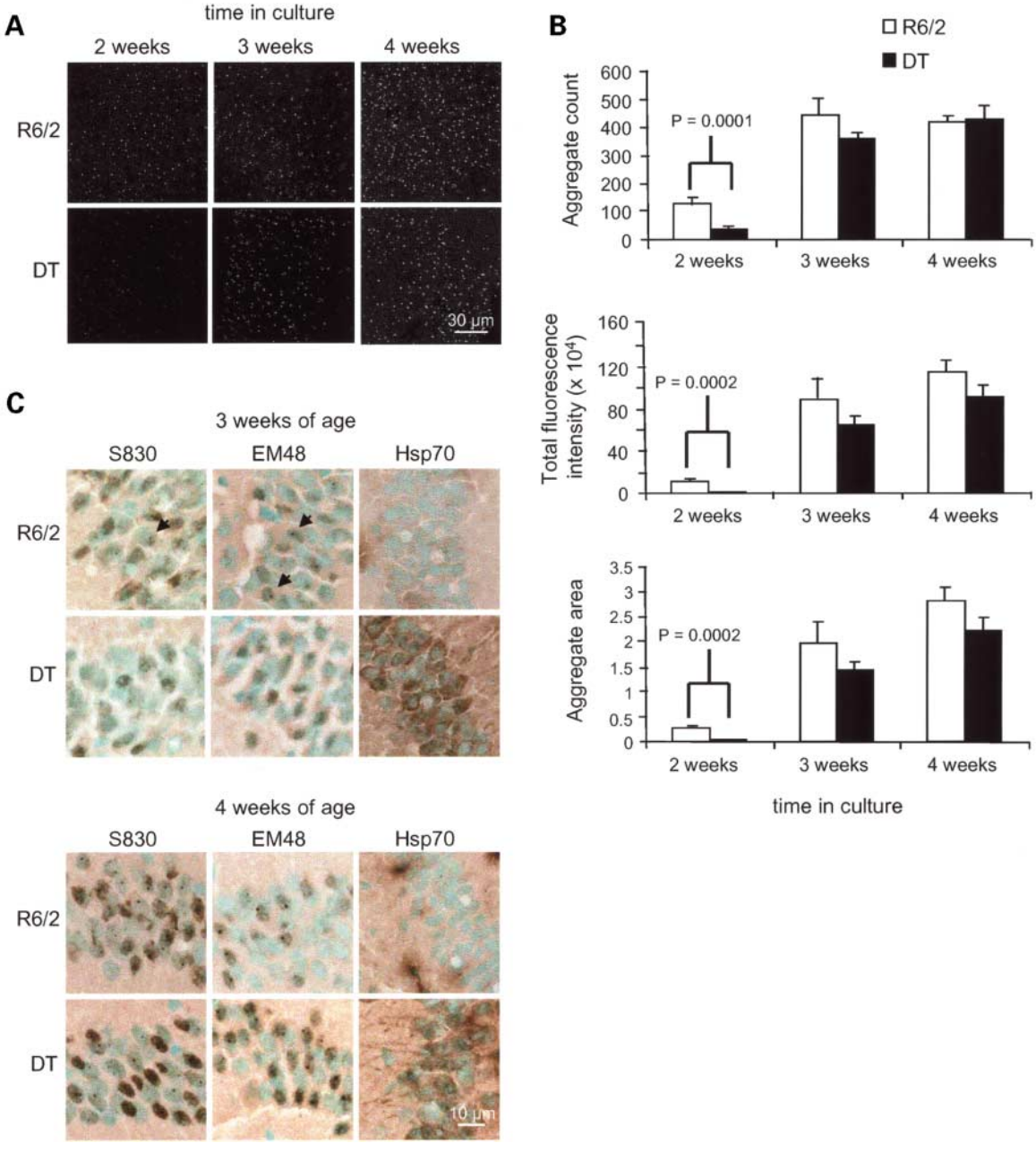


**Figure 4.** Overexpression of Hsp70 *in vivo* delays aggregate formation. (A, B) Hippocampal slices cultures were established from R6/2 and from double transgenic (DT) mice at 1 week of age. After 2, 3 and 4 weeks in culture, slices were fixed and the aggregate load in the CA1 region was quantified by indirect immunofluorescence and confocal microscopy. (**A**) Representative confocal images of the CA1 region after immunostaining with S830. Considerably fewer aggregates could be observed in slices from double transgenic mice after 2 weeks in culture (equivalent to 3 weeks *in vivo*) when compared with R6/2. After 3 and 4 weeks in culture no difference between number of aggregates in the double transgenic and R6/2 was apparent. (**B**) Quantification of the aggregate load in the double transgenic and R6/2 slices revealed a significant decrease after 2 weeks in culture but this effect had been lost after 3 weeks. The inhibition after 2 weeks was apparent by all measurement parameters (total number of aggregates, total fluorescent intensity of all aggregates, percentage area of the field occupied by aggregates). (**C**) Comparison of aggregate formation in brain sections from R6/2 and double transgenic (DT) mice taken at 3 and 4 weeks of age. At 3 weeks, inclusions can be detected in the CA1 pyramidal neurons in the R6/2 sections after immunostaining with both the S830 and EM48 antibodies (arrowheads) but not in sections from the double transgenic mice. At 4 weeks of age, aggregates are apparent in sections from both genotypes (equivalent to slices after 3 weeks in culture). Methyl green was used as a nuclear counterstain. This qualitative *in vivo* data is consistent with the results of the quantitative slice culture experiment.

of the measurement parameters used: number of aggregates ($P = 0.037$); total fluorescence intensity ($P = 0.005$); total aggregate area ($P = 0.006$) (Fig. 7A). This inhibitory effect was no longer present after 3 and 4 weeks in culture. This pattern of inhibition was mirrored when slices were treated with GA. No effect on aggregate load was observed in slices treated with 1 and 10 nM GA (data not shown). Exposure to 100 nM GA resulted in a significant decrease in aggregate

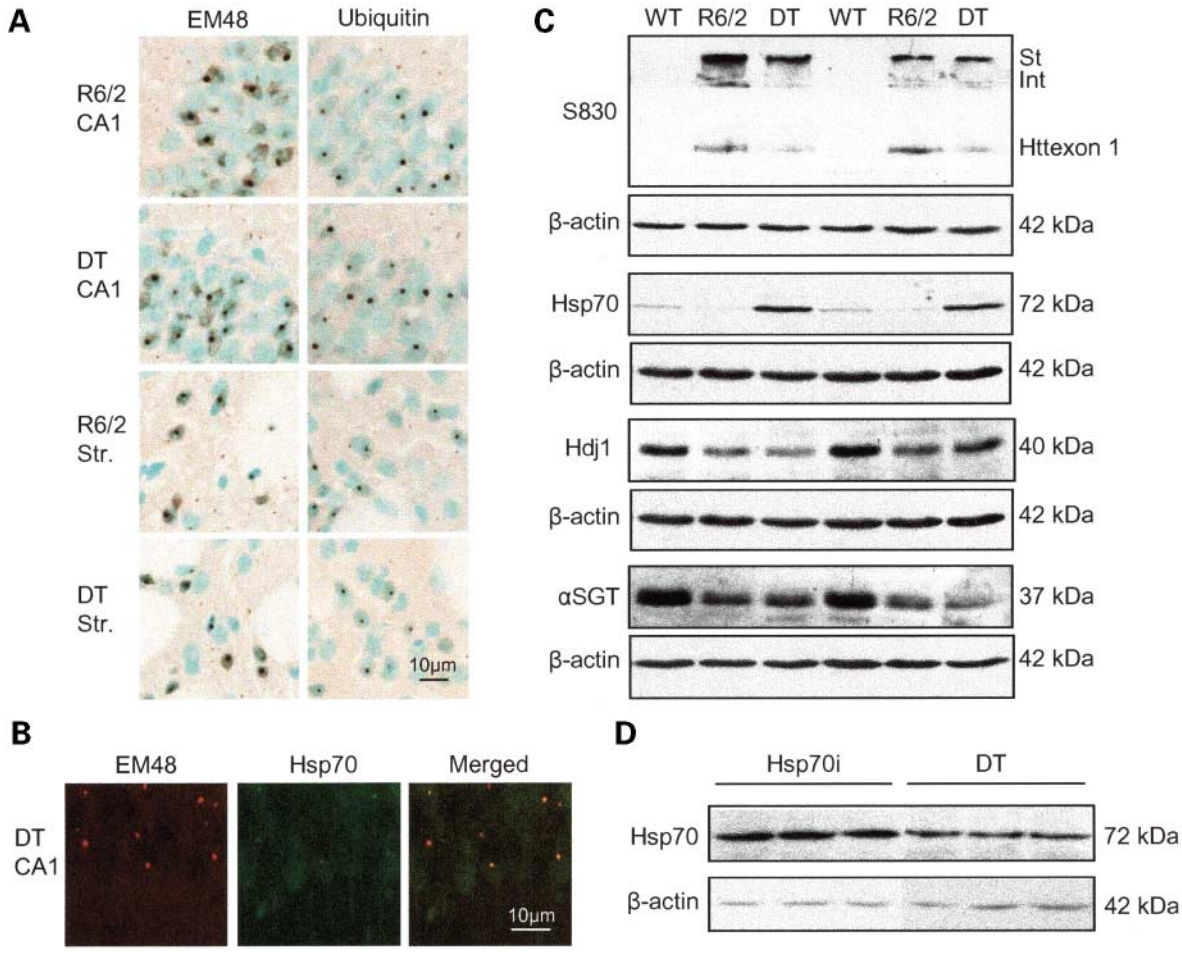


**Figure 5.** Overexpression of Hsp70 does not alter the progression of R6/2 pathogenesis. (**A**) Striatal (Str) and hippocampal (CA1) sections from R6/2 and double transgenic (DT) mice at 8 weeks of age immunoprobed with EM48 and anti-ubiquitin antibodies. There was no apparent difference in the number or appearance of the nuclear and extranuclear aggregates. Methyl green was used as a nuclear counterstain. (**B**) Hsp70 was found to co-localize with NIs in the CA1 hippocampal neurons in double transgenic (DT) mice. (**C**) Western blots of total brain lysates from mice at 12 weeks of age. The levels of soluble exon 1 huntingtin as detected by S830 are not increased in the double transgenic mice (DT) when compared with R6/2. Similarly, there is no consistent difference between the aggregated huntingtin that remains in the stacking gel. St = stacking gel; Int = interface between stacking and resolving gels. The expression of Hsp70 is much higher in the brains of the double transgenic mice than in wild-type or R6/2, in which it is barely detectable. The expression levels of Hdj1 and αSGT are decreased in R6/2 when compared with wild-type (WT) and remain decreased in the double transgenic (DT) mice. (**D**) Western blots of whole brain lysates from Hsp70i and double transgenic (DT) mice at 12 weeks of age. The level Hsp70 expressed by the transgene is lower in the double transgenics. Blots were reprobed with an antibody to β-actin to show relative loading levels.

load after 2 weeks in culture: number of aggregates, $P = 0.0082$; total fluorescence intensity, $P = 0.0004$; total aggregate area, $P = 0.0004$ (Fig. 7B), but this effect was not maintained after 3 and 4 weeks (data not shown). Finally, we compared the effects of the 10 μM RA constant and pulsed dosing regimes as described earlier. Constant exposure to 10 μM RA led to a significant decrease in aggregate load after 2 weeks: number of aggregates $P = 0.015$; total fluorescence intensity, $P = 0.001$; total aggregate area, $P = 0.003$ (Fig. 7C), verifying the results obtained in Figure 7A in an independent experiment, although once again, this effect was lost after 3 and 4 weeks in culture (data not shown). In contrast, pulsed dosing did not lead to a significant decrease in aggregation by any of the measurement parameters used (Fig. 7C).

In order to examine the effects of RA treatment on the levels of soluble exon 1 huntingtin, slices were treated with 10 μM RA by either the constant or pulsed dosing regimes or with vehicle as described earlier. Slices were harvested after 2, 3 and 4 weeks in culture, processed for western blotting and immunoprobed with antibodies to Hdj1, Hsp70 to monitor heat shock induction and with S830 to compare levels of soluble exon 1 huntingtin. Slices treated with 10 μM RA for 48 h were used as a positive control for heat shock induction. When compared with the vehicle control, treatment with 10 μM RA by either the pulsed or constant dosing regimes had no effect on the levels of soluble exon 1 huntingtin after the slices had been in culture for 2 weeks (1=week of treatment) (constant $P = 0.8$,

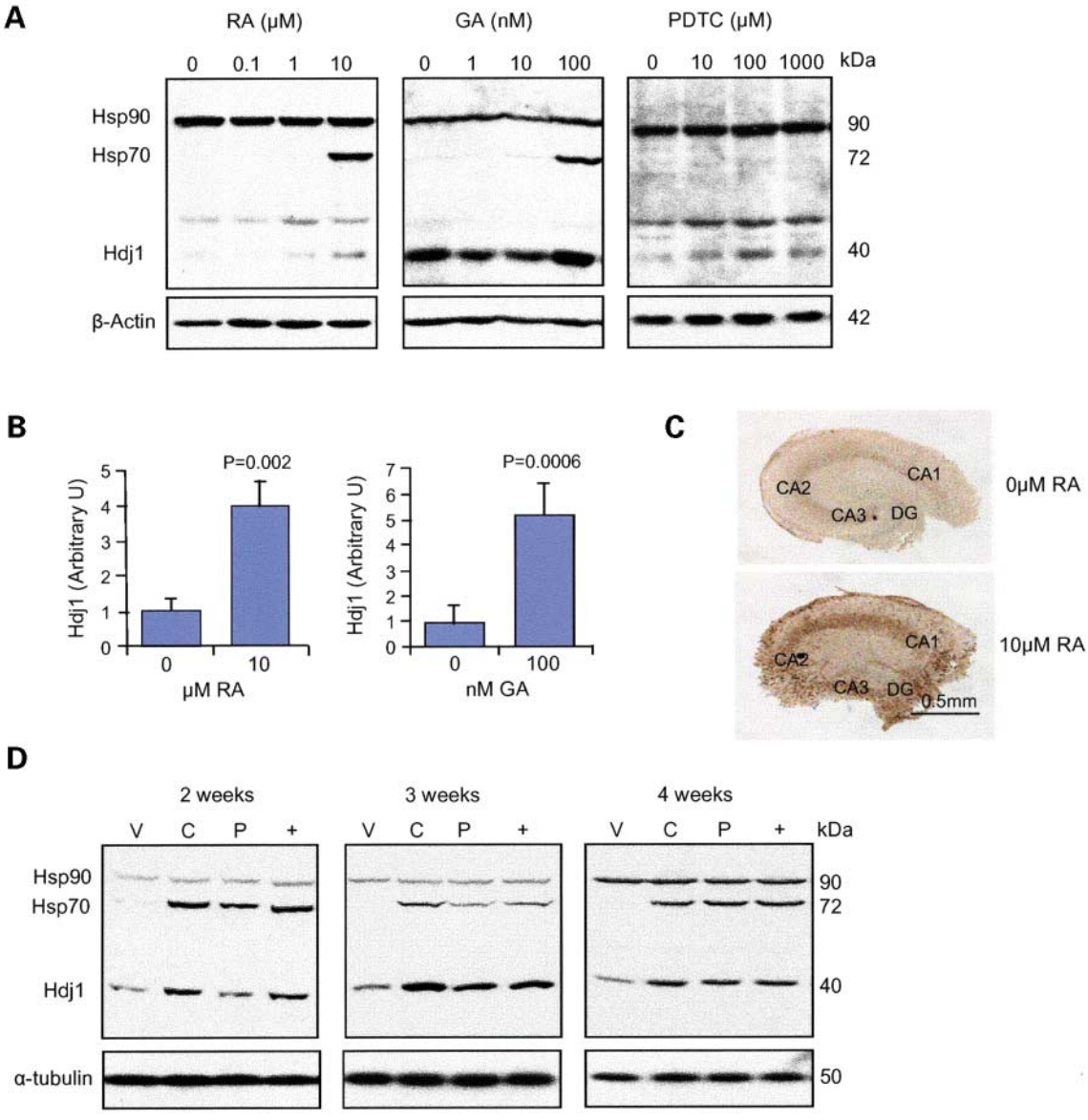


**Figure 6.** RA and GA induce the heat shock response in organotypic slice cultures. (**A**) Organotypic slices were established from R6/2 neonates at P7 and maintained in culture for 7 days and then exposed concentrations of RA, GA or PDTC for 48 h before harvesting and processing for western blotting. Induction of Hdj1 and Hsp70 was caused by treatment with 10 μM RA and 100 nM GA but not at lower concentration of these drugs. Hsp90 levels remained unchanged and PDTC did not induce a heat shock response at any of the concentrations tested. Blots were reprobed with an antibody to β-actin to show relative loading levels. (**B**) Semi-quantitative densitometric analysis of immunoblots of slices treated with either 10 μM RA or 100 nM GA for 48 h showed an increase of 4–5-fold in Hdj1 levels in treated when compared with untreated slices. (**C**) Slices cultured for 7 days and then treated with 10 μM RA for 48 h were processed for immunohistochemistry and immunoprobed with an antibody to Hsp70. Increased staining can be detected in the hippocampal neuronal layers of the treated when compared with the untreated slice. The counter stain is methyl green. (**D**) Qualitative comparison of the extent of heat shock induction in slices treated with 10 μM RA using either a constant or pulsed dosing regime. V = slices exposed to vehicle from 7 days in culture; C = slices exposed to 10 μM RA from 7 days in culture until harvesting after 2, 3 and 4 weeks in culture; P = slices exposed to 10 μM RA for 8 h every 4 days from 7 days in culture until harvesting after 2, 3 and 4 weeks in culture; + = slices exposed to 10 μM RA for 48 h to induce heat shock and act as a positive control. The constant and pulsed dosing regimes both maintained heat shock induction over the period of 3 weeks from commencement of treatment. Blots were reprobed with an antibody to α-tubulin to show relative loading levels.

pulsed $P = 0.41$). Only constant exposure to 10 μM RA resulted in an increase in soluble exon 1 huntingtin after 3 and 4 weeks in culture (Fig. 7D) when compared with the vehicle control (Student's *t*-test, $n = 3$, 3 weeks: constant $P < 0.001$, pulsed $P = 0.79$; 4 weeks: constant $P = 0.04$, pulsed $P = 0.33$).

## DISCUSSION

We have found that there is a progressive decrease in levels of specific chaperone proteins in the brains of R6/2 mice and propose that this is likely to contribute to the molecular pathogenesis of the disease. Hdj1, Hsp70, αSGT and βSGT are

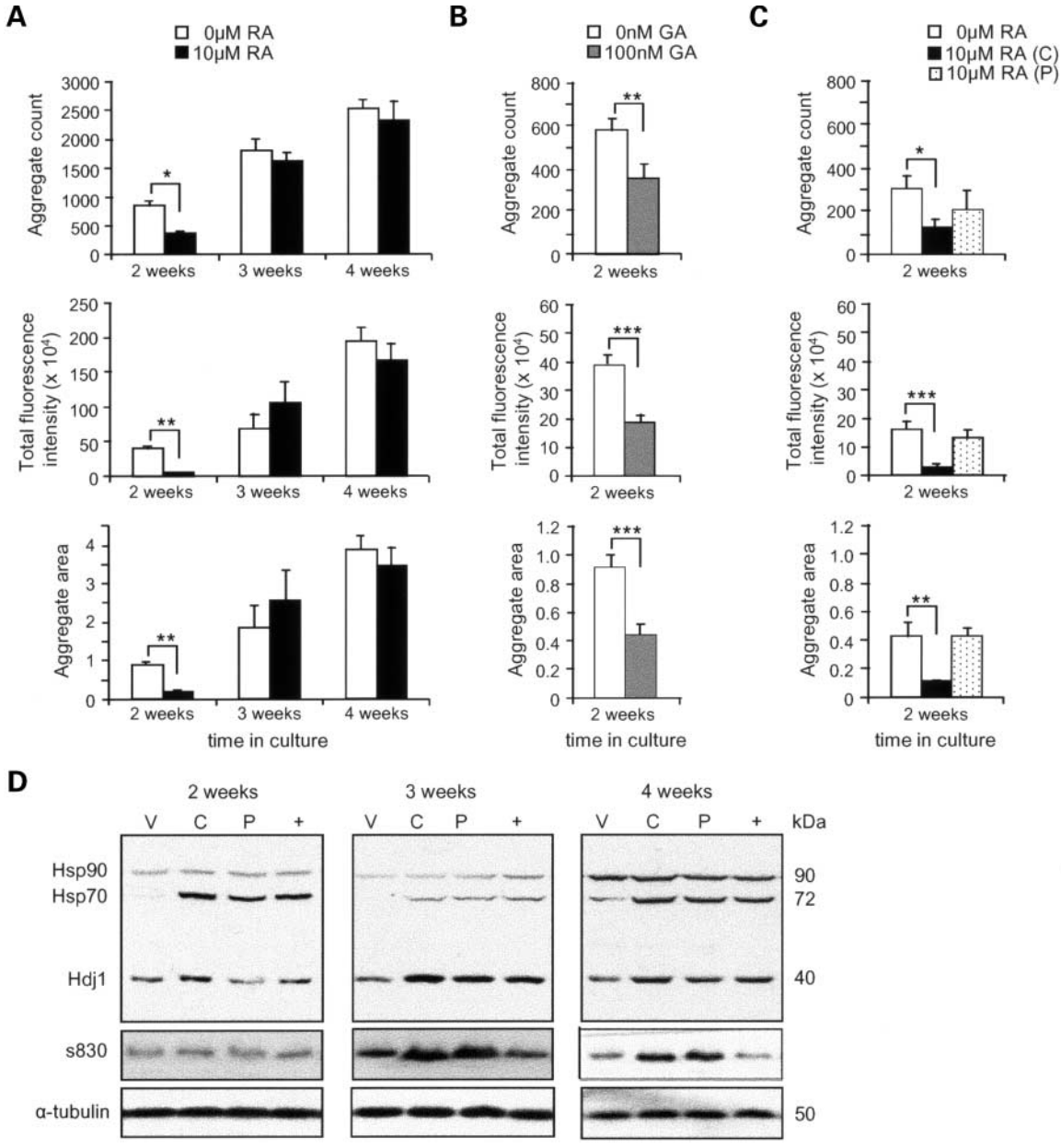


**Figure 7.** RA and GA delay aggregate formation in organotypic slice cultures and lead to an increase in levels of soluble exon 1 huntingtin. (**A**) Organotypic slices were established from R6/2 neonates at P7 and maintained in culture for 7 days and then exposed to 100 nM, 1 μM or 10 μM RA. Aggregate formation was delayed in slices treated with 10 μM radicicol in that the aggregate load was significantly decreased after 2 weeks in culture, but this effect had disappeared by 3 and 4 weeks. Aggregate formation was not influenced by treatment with 100 nM or 1 μM RA. (**B**) Similarly, treatment with 100 nM but not with 1 nM or 10 nM GA, significantly decreased aggregate load in the slice cultures after 2 weeks in culture, but had no effect after 3 and 4 weeks. (**C**) The aggregate load was significantly decreased in slices after 2 weeks in culture that had been exposed to a constant dosing regime (as in A), but not in those treated with a pulsed dosing regime of 10 μM RA for 8 h every 4 days. (**D**) Western blots showing heat shock induction and levels of soluble huntingtin exon 1 in slices that had been exposed to a constant or pulsed treatment regime with 10 μM RA. V = slices exposed to vehicle from 7 days in culture; C = slices exposed to 10 μM RA from 7 days in culture until harvesting after 2, 3 and 4 weeks in culture; P = slices exposed to 10 μM RA for 8 h every 4 days from 7 days in culture until harvesting after 2, 3 and 4 weeks in culture; + = slices exposed to 10 μM RA for 48 h to induce heat shock and act as a positive control. Prolonged treatment with 10 μM RA, whether by constant or by pulsed dosing led to an increase in levels of soluble huntingtin exon 1. Blots were reprobed with an antibody to α-tubulin to show relative loading levels. Error bars represent standard errors of the mean; $^{*}P \leq 0.05$, $^{**}P \leq 0.01$, $^{***}P \leq 0.001$.

already significantly decreased in whole brain lysates at 8 weeks and in all cases, are reduced to <40% of wild-type levels by 14 weeks. Hdj2 levels are also reduced, but to a lesser extent. A decrease in Hsp70 has been reported previously in the retina of R6/2, R6/1 and R7E SCA7 mice (56,57) and the authors suggested that this might be due to an impairment at the level of gene expression or of protein turnover. To explore this further, we quantified the mRNA levels of Hdj1 and αSGT and found no difference between R6/2 and wild-type brains at 14 weeks of age, indicating

that a defect at the level of transcription is unlikely. Instead, it was striking that a decrease in the amount of soluble protein correlated with the co-localization of that chaperone to nuclear inclusions and although Hsc70 provided an exception to this rule, Hsc70 accounts for a substantial fraction of CNS protein [2–3% of spinal cord total protein (58)] and this could mask any reduction in protein levels that are occurring. Therefore the recruitment of chaperones to polyQ aggregates might provide a plausible explanation for the decrease in the soluble protein levels. However, previous studies that have analysed the structure of polyQ aggregates (59) or the dynamics of the proteins that are associated with them (60) have concluded that Hsp70 is released from the aggregates in a monomeric form (59) and that the co-localization of Hsp70 with polyQ aggregates is indicative of chaperone–substrate interactions rather than sequestration (60). Although a more recent paper supports this by showing that Hsp70 is redistributed to the protease-sensitive shell of the huntingtin inclusion body, Hsp40 is contained within the protease-resistant core (61) indicating that sequestration may certainly account for the decrease in levels of the Hsp40 chaperones and possibly also αSGT and βSGT. It is also possible that the relocation to the nucleus enhances the turnover of these proteins. Although the subcellular localization of these chaperones is predominantly extranuclear, it is striking that co-localization is only seen with nuclear aggregates and not with extranuclear aggregates [(13), this paper]. The difference in the biochemical properties of nuclear and extranuclear aggregates responsible for this discrepancy is not understood.

This reduction in chaperone levels can be predicted to have a number of deleterious consequences. The co-operation of Hsp40 (Hdj1, Hdj2) and Hsp70 (Hsp70, Hsc70) chaperones is central to the ability of a cell to refold or degrade misfolded proteins (17). Prior to the initiation of the progressive decrease in Hsp70, Hdj1 and Hdj2 levels, the cellular capacity to prevent the accumulation of polyQ aggregates is already proving inadequate and this can only be exacerbated by a reduction in Hsp70/Hsp40 levels. Other consequences of a reduction in Hsp70 have already been explored in the cell culture systems and in the retina of R6/1 and R7E SCA7 mouse models (57). The authors proposed that the decrease in Hsp70 resulted in the aggregation and consequently the inhibition of the M3/6 JNK phosphatase leading to the activation of the stress kinase JNK and the transcription factor AP-1, which are involved in neuronal cell death (57). A polyQ-related reduction in the levels of αSGT and βSGT has not been reported previously. αSGT is a ubiquitously expressed co-chaperone of Hsc70 that forms a trimeric complex with Hsc70 and CSP located on the synaptic vesicle surface (62), and βSGT is a brain-specific isoform of αSGT with which it is likely to co-operate (63). CSP is also an Hsc70 co-chaperone that functions in the calcium activated exocytosis of synaptic vesicles (64,65). Although we did not see any evidence of CSP recruitment or reduction in our mouse model, *in vitro* and cell culture systems have recently shown that expanded polyQ can sequester CSP, block its association with G-proteins and modulate G-protein inhibition of calcium channel activity (66). Whether a decrease in αSGT and βSGT levels and/or an impairment of CSP function has an impact on synaptic transmission in the R6/2 mouse is yet to be investigated. However, SGT is a highly conserved protein (67) that clearly has important cellular functions other than its role in synaptic transmission and its reduction may have other deleterious consequences. In fact it has been shown recently that cells depleted of SGT are unable to complete cell division (68) and interestingly, this is a phenotype that we have described previously in fibroblast cultures derived from HD patients and R6/2 mice (69).

The use of mouse models to investigate the therapeutic potential of increasing chaperone levels has been restricted so far to crossing mice overexpressing Hsp70 to mouse models of SCA1 (32), HD [(34), this paper] and SBMA (33). Two Hsp70 transgenic mice have been used in these experiments: in one the human Hsp70 gene is expressed under the control of the human β-actin promoter (70) and in the second, the rat Hsp70 gene is expressed under the control of the chicken β-actin promoter and cytomegalovirus enhancer (51). Crossing the B05 mouse model of SCA1 to the rat Hsp70 transgenic mice resulted in a mild improvement in motor impairment and in Purkinje cell morphology, although the number of Purkinje cells containing nuclear inclusions remained the same (32). These effects might have been relatively mild because mutant ataxin 1 is overexpressed by 50–100-fold in the B05 line (50). In contrast, overexpression of human Hsp70 in SBMA mice caused a marked improvement in motor function and survival and delayed weight loss (33). This correlated with a significant reduction in the amount of mutant androgen receptor (AR) that was localized to the nucleus, particularly the large aggregated form that becomes trapped in the stacking gel on western blots and cellulose acetate membranes. It was notable that the level of monomeric mutant AR was also reduced, suggesting that Hsp70 not only decreased the large aggregated complexes but also enhanced the function of the ubiquitin–proteasome pathway and accelerated the degradation of the monomeric mutant AR protein (33).

Overexpression of Hsp70 in the R6/2 mouse model of HD has had a more disappointing outcome. Overexpression of human Hsp70 had no effect on R6/2 survival, paw clasping phenotype, the number and size of nuclear inclusions, loss of brain weight, striatal volume reduction, the decreased striatal projection neuron size or downregulation of DARPP32 (34). Similarly, we found that crossing R6/2 mice to the rat Hsp70 transgenic mice did not lead to an improvement in RotaRod performance, grip strength or weight loss. By using the organotypic slice culture system, we were able to show that overexpression of Hsp70 significantly delayed the formation of nuclear inclusions by approximately 1 week, i.e. they were present at 4 rather than at 3 weeks of age in the CA1 hippocampal neurons, but from 4 weeks onwards, no difference between the aggregate load in R6/2 and double transgenic mice could be detected. In addition, there was no difference in the detergent solubility of the nuclear aggregates at any age, as determined by western blotting. This early and transient inhibition of aggregate formation is consistent with *in vitro* data showing that Hsp70, in conjunction with Hsp40, only effectively inhibits polyQ fibril formation when added during the lag phase of the aggregation reaction (35) and that Hsp70 delays nucleation, but once seeding has occurred fails to inhibit polymerization. Also, in cell culture (19,20,22) and *Drosophila* (29) models of polyQ disease, the beneficial effects of Hsp70 have been enhanced when it is

overexpressed with its co-chaperone Hsp40. These chaperones have been shown to act in concert to alter the biochemical properties of the polyQ aggregates, converting them from detergent-insoluble inclusions to detergent-soluble amorphous structures (29,35) and *in vitro* experiments have shown that the ratio of Hsp40 to Hsp70 might be critical to this process (35). Therefore, the progressive decrease in Hdj1 and Hdj2 levels in the R6/2 mice (and possibly also that of αSGT and βSGT, and further as yet unidentified components of the stress response and protein folding machinery) might additionally compromise the ability of Hsp70 to solubilize and/or assist in the degradation of the mutant protein.

We hypothesized that exposure to drugs that induce the stress response by activating HSF1 and thereby increasing the expression of both Hsp40 and Hsp70 might be more effective at modulating the R6/2 phenotype. It had been shown already that GA induced expression of both Hsp40 and Hsp70 and consequently decreased polyQ aggregation in a cell culture model of HD (20). However, these experiments involved incubation with GA for <48 h and it was not clear that such drugs might be effective over a period of several weeks. As GA does not cross the blood–brain barrier, and RA has little or no activity in whole animals (71), we chose to use the organotypic slice culture system as a first step in the preclinical assessment of heat shock inducers as therapeutics for HD. We found that constant exposure to 100 nM GA and 10 μM RA successfully induced and maintained the expression of both Hsp40 (Hdj1) and Hsp70 over a period of at least 3 weeks. Pharmacological induction of the heat shock response delayed aggregate formation in the R6/2 brain slices by approximately 1 week, which was very similar to the effect achieved through Hsp70 overexpression in the R6/2::Hsp70i double transgenic mice. This delay in aggregate formation was caused by exposure to either GA or RA and only occurred at concentrations capable of inducing Hsp40 and Hsp70 expression. Pharmacological induction of the heat shock response also caused an increase in the level of soluble exon 1 huntingtin in the slice cultures as detected by western blot and in contrast to aggregate inhibition, this effect was still apparent in slices that had been exposed to drug for 3 weeks. This may indicate that chaperone induction has changed the biochemical properties of the aggregates, making them more detergent soluble akin to the effect observed previously in yeast, *Drosophila* and *in vitro* models (29,35,36). Given that a change in aggregate solubility was not detected in the R6/2::Hsp70i double transgenic mice, and that it is the change in the aggregate solubility that correlated with protection against neurotoxicity in *Drosophila* (29), we are optimistic that pharmacological induction of the heat shock response might be beneficial in a mouse model. The preclinical testing of novel compounds that induce the stress response and also cross the blood–brain barrier is worthwhile and should be pursued.

## MATERIALS AND METHODS

### Mouse models and husbandry

All mouse husbandry and experimental procedures complied with UK Home Office regulations. R6/2 mice (37) [available from the Induced Mutant Resource, Jackson Laboratory, Bar Harbor, ME, USA, code B6CBA-TgN (HDexon1)62] were bred by backcrossing R6/2 males to (CBA × C57BL/6) F1 females (Harlan Olac, Bichester, UK). R6/2 mice were identified prior to weaning by PCR of tail-tip DNA as described (39). Hsp70 mice were transgenic for the rat hsp70 gene driven by the β-actin promoter and chicken cytomegalovirus enhancer (51). Hemizygous mice overexpressing the inducible form of rat Hsp70 (Hsp70i) gene were identified by PCR of tail tip DNA as follows: 0.2 μg genomic DNA, 0.2 μg primers: GGAGGTGGATTAGAGGCTTT and ATCGATCCAGACATGATAAG, 0.5 mMdNTPs in 10 mM Tris–HCl (pH 9.2), 1.5 mM $MgCl_2$, 2.5 mM KCl, 5% formamide with 0.5 U *Taq* DNA polymerase (Applied Biosystems). Cycling conditions were (30 s at 94°C, 30 s at 50°C, 90 s at 72°C 90 s) × 30. Hsp70 males were bred to (CBA × C57BL/6) F1 females to generate hemizygous females for breeding to R6/2 males. All animals had unlimited access to water and to No. 3 rodent breeding chow (Special Diet Services, Witham, UK) from a food hopper. Mice were housed up to five per cage with a moderate level of environmental enrichment as described (39). The mice were subject to a 12 h light (08:00–20:00), 12 h dark (20:00–08:00) cycle.

### Phenotype analysis

RotaRod analysis was performed on an Ugo Basile 7650 accelerating RotaRod (Linton Instrumentation, UK), modified as described previously (39). At 4 weeks of age, mice were tested on four consecutive days, for three trials per day, while at 8 and 12 weeks, the mice were tested on three consecutive days, for three trials per day. Data from the first day of each time point (2 days at week 4) were not used in statistical analyses, as performance tends to improve as mice learn the task (39). Grip strength analysis was performed at 4, 8 and 12 weeks of age as described previously (39). Animals were weighed weekly to the nearest 0.1 g.

### RNA preparation and RQ-PCR

RNA for real-time quantitative PCR (RQ-PCR) was prepared from 30 mg cerebral cortex from animals at 14 weeks of age using the RNeasy kit (Qiagen). Reverse transcription of 1 μg of total RNA was as described previously (37) with the exception that reverse transcriptase (RT) was from Invitrogen. The RT reaction was diluted 2.5-fold in nuclease-free water (Sigma) and 5 μl was used in a 25 μl reaction containing Taqman master mix (ABI), 300 nM primers and 200 nM probe using the ABI7700 Taqman. Primer sequences for amplification of Hdj1 were 40450: CCCCATGCCATGTTT GCT and 40451: GCGCTGCCCAAAAAAGG and the probe was 40452: TCTTCGGTGGCAGAAACCCCTTTGA, Primer sequences for the amplification of SGT were 40400: GACAA CGGTGACCCGAGTGT and 40401: CGACGGAGAAAATG CTAAAACA and the probe was 40402: TTCGCTCCGCGG CCTCCTG. Primer sequences for amplification of β-actin were 40310: GCTTCTTTGCAGCTCCTTCGT and 40311: CCAGCGCAGCGATATCG and the probe was 40312: CGGT CCACACCCGCCACCAG. Primer sequences for the amplification of glutamate (NMDA) receptor subunit zeta 1 precursor (NR1) were 40325: TCAGTGTGTGAGGACCTCATCTCT and

40326: GAGTGAAGTGGTCGTTGGGAGTA and the probe was 40307: CAGGTCTACGCTATCCTAGTTAGTCACCCG CC. Estimation of mRNA copy number was determined in triplicate for each RNA sample through comparison with standard curves as described (72).

### Antibodies and western blotting

Whole brains were dissected from mice and rapidly frozen by immersion in dry-ice chilled isopentane. One-half brain was homogenized in 1 ml ice-cold RIPA buffer [150 mM NaCl, 50 mM Tris–HCl pH 7.4, 1% NP-40, 0.25% sodium deoxycholate, 0.2% sodium dodecyl sulfate (SDS), 1 mM EDTA, 1 mM phenylmethylsulfonyl fluoride (PMSF), complete protease inhibitors (Boehringer Mannheim)] using at least 10 strokes of a dounce homogenizer. The total protein concentration of the lysates was determined using the BCA assay kit (Perbio) and lysates were adjusted to 10 μg/μl total protein. Lysates were prepared from organotypic hippocampal slice cultures as follows: slices (typically 10) were rinsed with tris-buffered saline [0.1M Tris–HCl (pH 7.4), 0.9% NaCl], transferred to an Eppendorf tube and lysed by sonication in RIPA buffer (5 μl per slice) for 2 × 15 s using a Vibracell Sonicator (Sonics and Materials Inc. Danbury, CT, USA). Protein concentration was quantified using the BCA assay kit (Perbio) and adjusted to 1 μg/μl by addition of RIPA buffer. Nuclear and cytoplasmic fractions were prepared from snap-frozen whole brain according to a published protocol (73) except that the homogenate was not filtered through cheesecloth. The nuclear pellet was resuspended in 100 μl [575 mM sucrose, 25 mM KCl, 50 mM triethanolamine (pH 7.5), 5 mM $MgCl_2$, 1 mM dithiothreitol, 0.5 mM PMSF]. Lysates and nuclei and cytoplasmic preparations were aliquoted and stored at −80°C.

Freshly thawed lysates and cell fractions were quantified with the BCA protein assay kit (Perbio). Whole brain lysates (20–50 μg), slice culture lysates (20 μg) or nuclear (40–50 μg) and cytoplasmic (90–100 μg) fractions were loaded onto 10% SDS–PAGE gels, blotted onto Protran membranes (Schleicher and Schuell), immunoprobed and proteins detected as described (69). Primary antibodies and dilutions were: S830 (sheep pAb, 1:750) (69); Hdj1 (Stressgen SPA400, pAb, 1:5000); Hdj2 (Neomarkers Ab-1, mAb, 1:3000); Hsc70 (Santa Cruz Biotechnology SC-1059, goat pAb, 1:2000), Hsp70 (Stressgen SPA810, mAb, 1:1000), αβ-crystallin (Stressgen SPA223, pAb, 1:2000), Hsp25 (Stressgen SPA801, pAb, 1:2000), Hsp84 (Affinity Bioreagents Inc. PA3-012, pAb 1:2000), Hsp90 (Santa Cruz SC-7947, goat pAb, 1:2000), GRP78 (Transduction Laboratories, mAb, 1:500), αSGT (pAb 1:3000) (63), βSGT (pAb, 1:3000) (63), CSP (pAb 1:2000) (74), p60 (Stressgen SRA1500, mAb, 1:2000), α-tubulin (Sigma, mAb, 1:1000), β-actin (Abcam, mAb, 1:10 000). Horseradish peroxidase conjugated secondary antibody dilutions were: anti-rabbit (1:3000) (Dako), anti-sheep (1:3000) (Chemicon), anti-mouse (1:5000) (Vectastain). Digitized images of immunoreactive proteins were quantified using a KS300 image analysis system (Carl Zeiss Vision GmbH, Hallbergmoos, Germany).

### Immunohistochemistry and confocal microscopy

Animals were sacrificed by cervical dislocation, and brains were frozen immediately in isopentane and stored at −80°C. Sections of 15 μm thickness were cut using a cryostat (Bright Instrument Co. Ltd, UK). Immunohistochemistry for both light and confocal microscopy was performed as described previously (52). In addition to EM48 (pAb, 1:2000) (75) and ubiquitin (Dako, pAb, 1:1000), antibodies were as described above and used at the following dilutions: S830 (1:2000); Hdj1 (1:1000); Hdj2 (1:1000); Hsc70 (1:1000), Hsp70 (1:100), αβ-crystallin (1:1000), Hsp25 (1:1000), Hsp84 (1:1000), Hsp90 (1:1000), GRP78 (1:100), αSGT (1:1000), βSGT (1:500), CSP (1:1000), p60 (1:1000). Biotinylated secondary antibodies for light microscopy were from Vector Laboratories and used as follows: anti-sheep (1:500), anti-rabbit (1:200) and anti-mouse (1:500). Fluorescent secondary antibodies were from Molecular Probes and used as follows: Alex-488 anti goat (1:150), Alexa-488 anti-mouse (1:200), Alexa-546 anti-rabbit (1:400), Texas red anti-rabbit (1:300), Alex-594 anti-rabbit (1:250), and co-localization was determined using an LSM150 confocal microscope (Zeiss).

### Organotypic hippocampal slice culture assay

Hippocampal slice culture was performed as described previously (52). Transverse sections were dissected from R6/2 brains at 7 days of age, and established on Millicell-CM membranes (Sigma, Poole, UK) in Roth medium. GA (Sigma) was prepared at 1 mM in 100% dimethyl sulfoxide RA (Sigma) at 10 mM in 100% ethanol and PDTC (Sigma) at 1 M in water and stored at −20°C. To estimate heat shock induction, drugs were added to the medium and after the prescribed time interval slices were removed from the membrane and processed for western blotting. To quantify aggregate load, drugs were added to the culture medium after the slices had been cultured for 7 days and controls included slices incubated in Roth medium without supplements and in vehicle (0.01% DMSO or 0.1% ethanol). The medium (±drug) was changed twice weekly, and slices were taken for immunohistochemical analysis at weekly intervals from 2 to 4 weeks in culture. Huntingtin aggregate load was assessed by quantitative indirect immunofluorescence (52) and fluorescent confocal microscopy. Sections from all slices for the entire experiment were immunostained in parallel to minimize staining variation and the investigator was blind to genotype and time in culture until after all data collection. The total number of aggregates, total fluorescence intensity and the combined aggregate area (as a percentage of the total field) were calculated using a customized version of the KS-300 image analysis software package (Image Associates Ltd, Bicester, UK) for each concentration and each time point. All results were analysed by one-way ANOVA with false discovery rate (76) correction.

### Statistics

Student's *t*-test, general linear model (GLM) and one-way ANOVA were performed on Excel and Minitab.

## ACKNOWLEDGEMENTS

The authors wish to thank Anne McArdle for kindly providing the Hsp70 mice from her colony in Liverpool, Robert Burgoyne for generously providing the CSP antibody and Erich Wanker for discussions on geldanamycin. We also thank Emma Hockly for advice on statistics, Shabnam Ghaazi-Noori for advice on immunohistochemistry and confocal microscopy and Amy Barker and Jamie Tse for assistance with the mouse colony. This work was supported by a Medical Research Council studentship (D.H.) and by grants from the Wellcome Trust (60360; 66270), Medical Research Council (G9800001), Huntington's Disease Society of America Coalition for the Cure, Hereditary Disease Foundation and High Q Foundation.

## REFERENCES

1. Bates, G.P. and Benn, C. (2002) The polyglutamine diseases. In Bates, G.P., Harper, P.S. and Jones, A.L. (eds), *Huntington's Disease*, 3rd edn. Oxford University Press, Oxford, pp. 429–472.
2. Opal, P. and Zoghbi, H.Y. (2002) The role of chaperones in polyglutamine disease. *Trends Mol. Med.*, **8**, 232–236.
3. Ross, C.A. (2002) Polyglutamine pathogenesis: emergence of unifying mechanisms for Huntington's disease and related disorders. *Neuron*, **35**, 819–822.
4. Bates, G. (2003) Huntingtin aggregation and toxicity in Huntington's disease. *Lancet*, **361**, 1642–1644.
5. Fink, A.L. (1999) Chaperone-mediated protein folding. *Physiol. Rev.*, **79**, 425–449.
6. Hartl, F.U. and Hayer-Hartl, M. (2002) Molecular chaperones in the cytosol: from nascent chain to folded protein. *Science*, **295**, 1852–1858.
7. Bonifacino, J.S. and Weissman, A.M. (1998) Ubiquitin and the control of protein fate in the secretory and endocytic pathways. *Annu. Rev. Cell. Dev. Biol.*, **14**, 19–57.
8. Voges, D., Zwickl, P. and Baumeister, W. (1999) The 26S proteasome: a molecular machine designed for controlled proteolysis. *Annu. Rev. Biochem.*, **68**, 1015–1068.
9. Cummings, C.J., Mancini, M.A., Antalffy, B., DeFranco, D.B., Orr, H.T. and Zoghbi, H.Y. (1998) Chaperone suppression of aggregation and altered subcellular proteasome localization imply protein misfolding in SCA1. *Nat. Genet.*, **19**, 148–154.
10. Chai, Y., Koppenhafer, S.L., Bonini, N.M. and Paulson, H.L. (1999) Analysis of the role of heat shock protein (Hsp) molecular chaperones in polyglutamine disease. *J. Neurosci.*, **19**, 10338–10347.
11. Schmidt, T., Lindenberg, K.S., Krebs, A., Schols, L., Laccone, F., Herms, J., Rechsteiner, M., Riess, O. and Landwehrmeyer, G.B. (2002) Protein surveillance machinery in brains with spinocerebellar ataxia type 3: redistribution and differential recruitment of 26S proteasome subunits and chaperones to neuronal intranuclear inclusions. *Ann. Neurol.*, **51**, 302–310.
12. Yvert, G., Lindenberg, K.S., Picaud, S., Landwehrmeyer, G.B., Sahel, J.A. and Mandel, J.L. (2000) Expanded polyglutamines induce neurodegeneration and trans-neuronal alterations in cerebellum and retina of SCA7 transgenic mice. *Hum. Mol. Genet.*, **9**, 2491–2506.
13. Jana, N.R., Tanaka, M., Wang, G. and Nukina, N. (2000) Polyglutamine length-dependent interaction of Hsp40 and Hsp70 family chaperones with truncated N-terminal huntingtin: their role in suppression of aggregation and cellular toxicity. *Hum. Mol. Genet.*, **9**, 2009–2018.
14. Mitsui, K., Nakayama, H., Akagi, T., Nekooki, M., Ohtawa, K., Takio, K., Hashikawa, T. and Nukina, N. (2002) Purification of polyglutamine aggregates and identification of elongation factor-1alpha and heat shock protein 84 as aggregate-interacting proteins. *J. Neurosci.*, **22**, 9267–9277.
15. Ishihara, K., Yamagishi, N., Saito, Y., Adachi, H., Kobayashi, Y., Sobue, G., Ohtsuka, K. and Hatayama, T. (2003) Hsp105alpha suppresses the aggregation of truncated androgen receptor with expanded CAG repeats and cell toxicity. *J. Biol. Chem.*, **278**, 25143–25150.
16. Sherman, M.Y. and Goldberg, A.L. (2001) Cellular defenses against unfolded proteins: a cell biologist thinks about neurodegenerative diseases. *Neuron*, **29**, 15–32.
17. Sakahira, H., Breuer, P., Hayer-Hartl, M.K. and Hartl, F.U. (2002) Molecular chaperones as modulators of polyglutamine protein aggregation and toxicity. *Proc. Natl Acad. Sci. USA*, **99**, 16412–16418.
18. Stenoien, D.L., Cummings, C.J., Adams, H.P., Mancini, M.G., Patel, K., DeMartino, G.N., Marcelli, M., Weigel, N.L. and Mancini, M.A. (1999) Polyglutamine-expanded androgen receptors form aggregates that sequester heat shock proteins, proteasome components and SRC-1, and are suppressed by the HDJ-2 chaperone. *Hum. Mol. Genet.*, **8**, 731–741.
19. Kobayashi, Y., Kume, A., Li, M., Doyu, M., Hata, M., Ohtsuka, K. and Sobue, G. (2000) Chaperones Hsp70 and Hsp40 suppress aggregate formation and apoptosis in cultured neuronal cells expressing truncated androgen receptor protein with expanded polyglutamine tract. *J. Biol. Chem.*, **275**, 8772–8778.
20. Sittler, A., Lurz, R., Lueder, G., Priller, J., Hayer-Hartl, M.K., Hartl, F.U., Lehrach, H. and Wanker, E.E. (2001) Geldanamycin activates a heat shock response and inhibits huntingtin aggregation in a cell culture model of Huntington's disease. *Hum. Mol. Genet.*, **10**, 1307–1315.
21. Zhou, H., Li, S.H. and Li, X.J. (2001) Chaperone suppression of cellular toxicity of huntingtin is independent of polyglutamine aggregation. *J. Biol. Chem.*, **276**, 48417–48424.
22. Bailey, C.K., Andriola, I.F., Kampinga, H.H. and Merry, D.E. (2002) Molecular chaperones enhance the degradation of expanded polyglutamine repeat androgen receptor in a cellular model of spinal and bulbar muscular atrophy. *Hum. Mol. Genet.*, **11**, 515–523.
23. Wyttenbach, A., Carmichael, J., Swartz, J., Furlong, R.A., Narain, Y., Rankin, J. and Rubinsztein, D.C. (2000) Effects of heat shock, heat shock protein 40 (HDJ-2), and proteasome inhibition on protein aggregation in cellular models of Huntington's disease. *Proc. Natl Acad. Sci. USA*, **97**, 2898–2903.
24. Chuang, J.Z., Zhou, H., Zhu, M., Li, S.H., Li, X.J. and Sung, C.H. (2002) Characterization of a brain-enriched chaperone, MRJ, that inhibits huntingtin aggregation and toxicity independently. *J. Biol. Chem.*, **277**, 19831–19838.
25. Carmichael, J., Chatellier, J., Woolfson, A., Milstein, C., Fersht, A.R. and Rubinsztein, D.C. (2000) Bacterial and yeast chaperones reduce both aggregate formation and cell death in mammalian cell models of Huntington's disease. *Proc. Natl Acad. Sci. USA*, **97**, 9701–9705.
26. Wyttenbach, A., Sauvageot, O., Carmichael, J., Diaz-Latoud, C., Arrigo, A.P. and Rubinsztein, D.C. (2002) Heat shock protein 27 prevents cellular polyglutamine toxicity and suppresses the increase of reactive oxygen species caused by huntingtin. *Hum. Mol. Genet.*, **11**, 1137–1151.
27. Satyal, S.H., Schmidt, E., Kitagawa, K., Sondheimer, N., Lindquist, S., Kramer, J.M. and Morimoto, R.I. (2000) Polyglutamine aggregates alter protein folding homeostasis in *Caenorhabditis elegans. Proc. Natl Acad. Sci. USA*, **97**, 5750–5755.
28. Warrick, J.M., Chan, H.Y., Gray-Board, G.L., Chai, Y., Paulson, H.L. and Bonini, N.M. (1999) Suppression of polyglutamine-mediated neurodegeneration in *Drosophila* by the molecular chaperone HSP70. *Nat. Genet.*, **23**, 425–428.
29. Chan, H.Y., Warrick, J.M., Gray-Board, G.L., Paulson, H.L. and Bonini, N.M. (2000) Mechanisms of chaperone suppression of polyglutamine disease: selectivity, synergy and modulation of protein solubility in *Drosophila. Hum. Mol. Genet.*, **9**, 2811–2820.
30. Kazemi-Esfarjani, P. and Benzer, S. (2000) Genetic suppression of polyglutamine toxicity in *Drosophila. Science*, **287**, 1837–1840.
31. Fernandez-Funez, P., Nino-Rosales, M.L., de Gouyon, B., She, W.C., Luchak, J.M., Martinez, P., Turiegano, E., Benito, J., Capovilla, M., Skinner, P.J. *et al.* (2000) Identification of genes that modify ataxin-1-induced neurodegeneration. *Nature*, **408**, 101–106.
32. Cummings, C.J., Sun, Y., Opal, P., Antalffy, B., Mestril, R., Orr, H.T., Dillmann, W.H. and Zoghbi, H.Y. (2001) Over-expression of inducible HSP70 chaperone suppresses neuropathology and improves motor function in SCA1 mice. *Hum. Mol. Genet.*, **10**, 1511–1518.
33. Adachi, H., Katsuno, M., Minamiyama, M., Sang, C., Pagoulatos, G., Angelidis, C., Kusakabe, M., Yoshiki, A., Kobayashi, Y., Doyu, M. *et al.* (2003) Heat shock protein 70 chaperone overexpression ameliorates phenotypes of the spinal and bulbar muscular atrophy transgenic mouse model by reducing nuclear-localized mutant androgen receptor protein. *J. Neurosci.*, **23**, 2203–2211.
34. Hansson, O., Nylandsted, J., Castilho, R.F., Leist, M., Jaattela, M. and Brundin, P. (2003) Overexpression of heat shock protein 70 in R6/2 Huntington's disease mice has only modest effects on disease progression. *Brain Res.*, **970**, 47–57.

35. Muchowski, P.J., Schaffar, G., Sittler, A., Wanker, E.E., Hayer-Hartl, M.K. and Hartl, F.U. (2000) Hsp70 and hsp40 chaperones can inhibit self-assembly of polyglutamine proteins into amyloid-like fibrils. *Proc. Natl Acad. Sci. USA*, **97**, 7841–7846.
36. Krobitsch, S. and Lindquist, S. (2000) Aggregation of huntingtin in yeast varies with the length of the polyglutamine expansion and the expression of chaperone proteins. *Proc. Natl Acad. Sci. USA*, **97**, 1589–1594.
37. Mangiarini, L., Sathasivam, K., Seller, M., Cozens, B., Harper, A., Hetherington, C., Lawton, M., Trottier, Y., Lehrach, H., Davies, S.W. *et al.* (1996) Exon 1 of the HD gene with an expanded CAG repeat is sufficient to cause a progressive neurological phenotype in transgenic mice. *Cell*, **87**, 493–506.
38. Davies, S.W., Turmaine, M., Cozens, B.A., DiFiglia, M., Sharp, A.H., Ross, C.A., Scherzinger, E., Wanker, E.E., Mangiarini, L. and Bates, G.P. (1997) Formation of neuronal intranuclear inclusions underlies the neurological dysfunction in mice transgenic for the HD mutation. *Cell*, **90**, 537–548.
39. Hockly, E., Woodman, B., Mahal, A., Lewis, C.M. and Bates, G. (2003) Standardization and statistical approaches to therapeutic trials in the R6/2 mouse. *Brain Res. Bull.*, **61**, 469–479.
40. Li, H., Li, S.H., Cheng, A.L., Mangiarini, L., Bates, G.P. and Li, X.J. (1999) Ultrastructural localization and progressive formation of neuropil aggregates in Huntington's disease transgenic mice. *Hum. Mol. Genet.*, **8**, 1227–1236.
41. Morton, A.J., Lagan, M.A., Skepper, J.N. and Dunnett, S.B. (2000) Progressive formation of inclusions in the striatum and hippocampus of mice transgenic for the human Huntington's disease mutation. *J. Neurocytol.*, **29**, 679–702.
42. Carter, R.J., Lione, L.A., Humby, T., Mangiarini, L., Mahal, A., Bates, G.P., Dunnett, S.B. and Morton, A.J. (1999) Characterization of progressive motor deficits in mice transgenic for the human Huntington's disease mutation. *J. Neurosci.*, **19**, 3248–3257.
43. Lione, L.A., Carter, R.J., Hunt, M.J., Bates, G.P., Morton, A.J. and Dunnett, S.B. (1999) Selective discrimination learning impairments in mice expressing the human Huntington's disease mutation. *J. Neurosci.*, **19**, 10428–10437.
44. Zabel, C., Chamrad, D.C., Priller, J., Woodman, B., Meyer, H.E., Bates, G.P. and Klose, J. (2002) Alterations in the mouse and human proteome caused by Huntington's disease. *Mol. Cell Proteomics*, **1**, 366–375.
45. Cha, J.H. (2000) Transcriptional dysregulation in Huntington's disease. *Trends Neurosci.*, **23**, 387–392.
46. Sugars, K.L. and Rubinsztein, D.C. (2003) Transcriptional abnormalities in Huntington disease. *Trends Genet.*, **19**, 233–238.
47. Zuccato, C., Tartari, M., Crotti, A., Goffredo, D., Valenza, M., Conti, L., Cataudella, T., Leavitt, B.R., Hayden, M.R., Timmusk, T. *et al.* (2003) Huntingtin interacts with REST/NRSF to modulate the transcription of NRSE-controlled neuronal genes. *Nat. Genet.*, **35**, 76–83.
48. Glass, M., Dragunow, M. and Faull, R.L. (2000) The pattern of neurodegeneration in Huntington's disease: a comparative study of cannabinoid, dopamine, adenosine and GABA(A) receptor alterations in the human basal ganglia in Huntington's disease. *Neuroscience*, **97**, 505–519.
49. Luthi-Carter, R., Strand, A., Peters, N.L., Solano, S.M., Hollingsworth, Z.R., Menon, A.S., Frey, A.S., Spektor, B.S., Penney, E.B., Schilling, G. *et al.* (2000) Decreased expression of striatal signaling genes in a mouse model of Huntington's disease. *Hum. Mol. Genet.*, **9**, 1259–1271.
50. Burright, E.N., Clark, H.B., Servadio, A., Matilla, T., Feddersen, R.M., Yunis, W.S., Duvick, L.A., Zoghbi, H.Y. and Orr, H.T. (1995) SCA1 transgenic mice: a model for neurodegeneration caused by an expanded CAG trinucleotide repeat. *Cell*, **82**, 937–948.
51. Marber, M.S., Mestril, R., Chi, S.H., Sayen, M.R., Yellon, D.M. and Dillmann, W.H. (1995) Overexpression of the rat inducible 70-kD heat stress protein in a transgenic mouse increases the resistance of the heart to ischemic injury. *J. Clin. Invest.*, **95**, 1446–1456.
52. Smith, D.L., Portier, R., Woodman, B., Hockly, E., Mahal, A., Klunk, W.E., Li, X.J., Wanker, E., Murray, K.D. and Bates, G.P. (2001) Inhibition of polyglutamine aggregation in R6/2 HD brain slices—complex dose–response profiles. *Neurobiol. Dis.*, **8**, 1017–1026.
53. Auluck, P.K. and Bonini, N.M. (2002) Pharmacological prevention of Parkinson disease in *Drosophila*. *Nat. Med.*, **8**, 1185–1186.
54. Schulte, T.W., Akinaga, S., Soga, S., Sullivan, W., Stensgard, B., Toft, D. and Neckers, L.M. (1998) Antibiotic radicicol binds to the N-terminal domain of Hsp90 and shares important biologic activities with geldanamycin. *Cell Stress Chaperones*, **3**, 100–108.
55. Kim, S.H., Han, S.I., Oh, S.Y., Chung, H.Y., Kim, H.D. and Kang, H.S. (2001) Activation of heat shock factor 1 by pyrrolidine dithiocarbamate is mediated by its activities as pro-oxidant and thiol modulator. *Biochem. Biophys. Res. Commun.*, **281**, 367–372.
56. Helmlinger, D., Yvert, G., Picaud, S., Merienne, K., Sahel, J., Mandel, J.L. and Devys, D. (2002) Progressive retinal degeneration and dysfunction in R6 Huntington's disease mice. *Hum. Mol. Genet.*, **11**, 3351–3359.
57. Merienne, K., Helmlinger, D., Perkin, G.R., Devys, D. and Trottier, Y. (2003) Polyglutamine expansion induces a protein-damaging stress connecting heat shock protein 70 to the JNK pathway. *J. Biol. Chem.*, **278**, 16957–16967.
58. Aquino, D.A., Klipfel, A.A., Brosnan, C.F. and Norton, W.T. (1993) The 70-kDa heat shock cognate protein (HSC70) is a major constituent of the central nervous system and is up-regulated only at the mRNA level in acute experimental autoimmune encephalomyelitis. *J. Neurochem.*, **61**, 1340–1348.
59. Suhr, S.T., Senut, M.C., Whitelegge, J.P., Faull, K.F., Cuizon, D.B. and Gage, F.H. (2001) Identities of sequestered proteins in aggregates from cells with induced polyglutamine expression. *J. Cell Biol.*, **153**, 283–294.
60. Kim, S., Nollen, E.A., Kitagawa, K., Bindokas, V.P. and Morimoto, R.I. (2002) Polyglutamine protein aggregates are dynamic. *Nat. Cell Biol.*, **4**, 826–831.
61. Qin, Z.H., Wang, Y., Sapp, E., Cuiffo, B., Wanker, E., Hayden, M.R., Kegel, K.B., Aronin, N. and DiFiglia, M. (2004) Huntingtin bodies sequester vesicle-associated proteins by a polyproline-dependent interaction. *J. Neurosci.*, **24**, 269–281.
62. Tobaben, S., Thakur, P., Fernandez-Chacon, R., Sudhof, T.C., Rettig, J. and Stahl, B. (2001) A trimeric protein complex functions as a synaptic chaperone machine. *Neuron*, **31**, 987–999.
63. Tobaben, S., Varoqueaux, F., Brose, N., Stahl, B. and Meyer, G. (2003) A brain-specific isoform of small glutamine-rich tetratricopeptide repeat-containing protein binds to Hsc70 and the cysteine string protein. *J. Biol. Chem.*, **278**, 38376–38383.
64. Zinsmaier, K.E., Eberle, K.K., Buchner, E., Walter, N. and Benzer, S. (1994) Paralysis and early death in cysteine string protein mutants of *Drosophila*. *Science*, **263**, 977–980.
65. Mastrogiacomo, A., Parsons, S.M., Zampighi, G.A., Jenden, D.J., Umbach, J.A. and Gundersen, C.B. (1994) Cysteine string proteins: a potential link between synaptic vesicles and presynaptic $Ca^{2+}$ channels. *Science*, **263**, 981–982.
66. Miller, L.C., Swayne, L.A., Chen, L., Feng, Z.P., Wacker, J.L., Muchowski, P.J., Zamponi, G.W. and Braun, J.E. (2003) Cysteine string protein (CSP) inhibition of N-type calcium channels is blocked by mutant huntingtin. *J. Biol. Chem.*, **278**, 53072–53081.
67. Kordes, E., Savelyeva, L., Schwab, M., Rommelaere, J., Jauniaux, J.C. and Cziepluch, C. (1998) Isolation and characterization of human SGT and identification of homologues in *Saccharomyces cerevisiae* and *Caenorhabditis elegans*. *Genomics*, **52**, 90–94.
68. Winnefeld, M., Rommelaere, J. and Cziepluch, C. (2004) The human small glutamine-rich TPR-containing protein is required for progress through cell division. *Exp. Cell Res.*, **293**, 43–57.
69. Sathasivam, K., Woodman, B., Mahal, A., Bertaux, F., Wanker, E.E., Shima, D.T. and Bates, G.P. (2001) Centrosome disorganization in fibroblast cultures derived from R6/2 Huntington's disease (HD) transgenic mice and HD patients. *Hum. Mol. Genet.*, **10**, 2425–2435.
70. Plumier, J.C., Ross, B.M., Currie, R.W., Angelidis, C.E., Kazlaris, H., Kollias, G. and Pagoulatos, G.N. (1995) Transgenic mice expressing the human heat shock protein 70 have improved post-ischemic myocardial recovery. *J. Clin. Invest.*, **95**, 1854–1860.
71. Soga, S., Neckers, L.M., Schulte, T.W., Shiotsu, Y., Akasaka, K., Narumi, H., Agatsuma, T., Ikuina, Y., Murakata, C., Tamaoki, T. *et al.* (1999) KF25706, a novel oxime derivative of radicicol, exhibits *in vivo* antitumor activity via selective depletion of Hsp90 binding signaling molecules. *Cancer Res.*, **59**, 2931–2938.

72. Grimwade, D., Outram, S.V., Flora, R., Ings, S.J., Pizzey, A.R., Morilla, R., Craddock, C.F., Linch, D.C. and Solomon, E. (2002) The T-lineage-affiliated CD2 gene lies within an open chromatin environment in acute promyelocytic leukemia cells. *Cancer Res.*, **62**, 4730–4735.
73. Hallberg, E. (1994) Preparation of nuclei and nuclear envelopes: identification of an integral membrane protein unique to the nuclear envelope. In Celis, J.E. (ed.), *Cell Biology: A Laboratory Handbook.* Academic Press, San Diego, Vol. 1, pp. 613–627.
74. Chamberlain, L.H. and Burgoyne, R.D. (1996) Identification of a novel cysteine string protein variant and expression of cysteine string proteins in non-neuronal cells. *J. Biol. Chem.*, **271**, 7320–7323.
75. Li, S.H. and Li, X.J. (1998) Aggregation of N-terminal huntingtin is dependent on the length of its glutamine repeats. *Hum. Mol. Genet.*, **7**, 777–782.
76. Hochberg, Y. and Benjamini, Y. (1990) More powerful procedures for multiple significance testing. *Stat. Med.*, **9**, 811–818.